Hindawi
Discrete Dynamics in Nature and Society
Volume 2020, Article ID 4561241, 20 pages
https://doi.org/10.1155/2020/4561241

Research Article

The Impulsive Model with Pest Density and Its Change Rate Dependent Feedback Control

Ihsan Ullah Khan and Sanyi Tang

School of Mathematics and Information Science, Shaanxi Normal University, Xi'an 710062, China

Correspondence should be addressed to Sanyi Tang; sytang@snnu.edu.cn

Received 23 June 2019; Revised 13 September 2019; Accepted 27 September 2019; Published 21 February 2020

Academic Editor: Nickolai Kosmatov

The idea of action threshold depends on the pest density and its change rate is more general and furthermore can produce new modelling techniques related to integrated pest management (IPM) as compared with those that appeared in earlier studies, which definitely bring challenges to analytical analysis and generate new ideas to the state control measures. Keeping this in mind, using the strategies of IPM, we develop a prey-predator system with action threshold depending on the pest density and its change rate, and study its dynamical behavior. We develop new criteria guaranteeing the existence, uniqueness, local and global stability of order-1 periodic solutions. Applying the properties of Lambert W function, the Poincaré map is portrayed for the exact phase set, which is helpful to provide the sufficient conditions for the existence and stability of the interior order-1 periodic solutions and boundary order-1 periodic solution, also confirmed by numerical simulations. It is studied in detail that how and under what conditions the fixed point of Poincaré map and its stability are affected by the newly introduced action threshold. The analytical methods developed in this paper will be very beneficial to study other generalized models with state-dependent feedback control.

1. Introduction

The risk of pests to agricultural productions may be an enormous issue over the world, which makes pest control being a motivating topic and attracts great attention to the development of effective pest management strategies. Pests will cause vital crop yield declines, even colossal failure. Additionally, they will downsize the standard of farm items. Therefore, countries around the world have established special organizations to review the management procedure of agricultural pests [1–7].

Integrated pest management (IPM) is a useful methodology in prevailing pests that have been demonstrated to be more practical than the classic strategies both experimentally [8–10] and theoretically [11, 12]. It is a procedure that is used to solve pest problems while minimizing threats to individuals and the environment. IPM can be utilized to deal with all sorts of pests anywhere in rural, urban, and natural areas or wild land. IPM is an ecosystem-based approach that concentrates on long-term prevention of pests or their damage through a combination of strategies, such as biological control, adjustment of social practices, living space control, and utilization of safe assortments. The objective of IPM is not to eliminate pests, rather to manage the amount of the pests below an associated economic threshold (ET) and ensure ecosystem up to maximum level.

Recently, many researchers have proposed impulsive differential equations to examine the dynamics of pest control models [13–18]. Impulsive equations have been brought into population dynamics in relation to impulsive vaccination, chemotherapeutic handling of disease, population ecology, and impulsive birth. Especially, some impulsive differential equations have been presented effectively in population dynamics (agriculture or fishing) and epidemic dynamics. Numerous recent articles have mathematically exhibited a variety of IPM tactics using impulsive differential equations, for example, stage structure in the predator species and periodically changing environmental conditions [19]. Relative models also have been studied in [20].

Most of the researchers considered systems with impulses at fixed moments [21–29]. The shortcomings of this kind of systems are that they did not pay enough attention to the

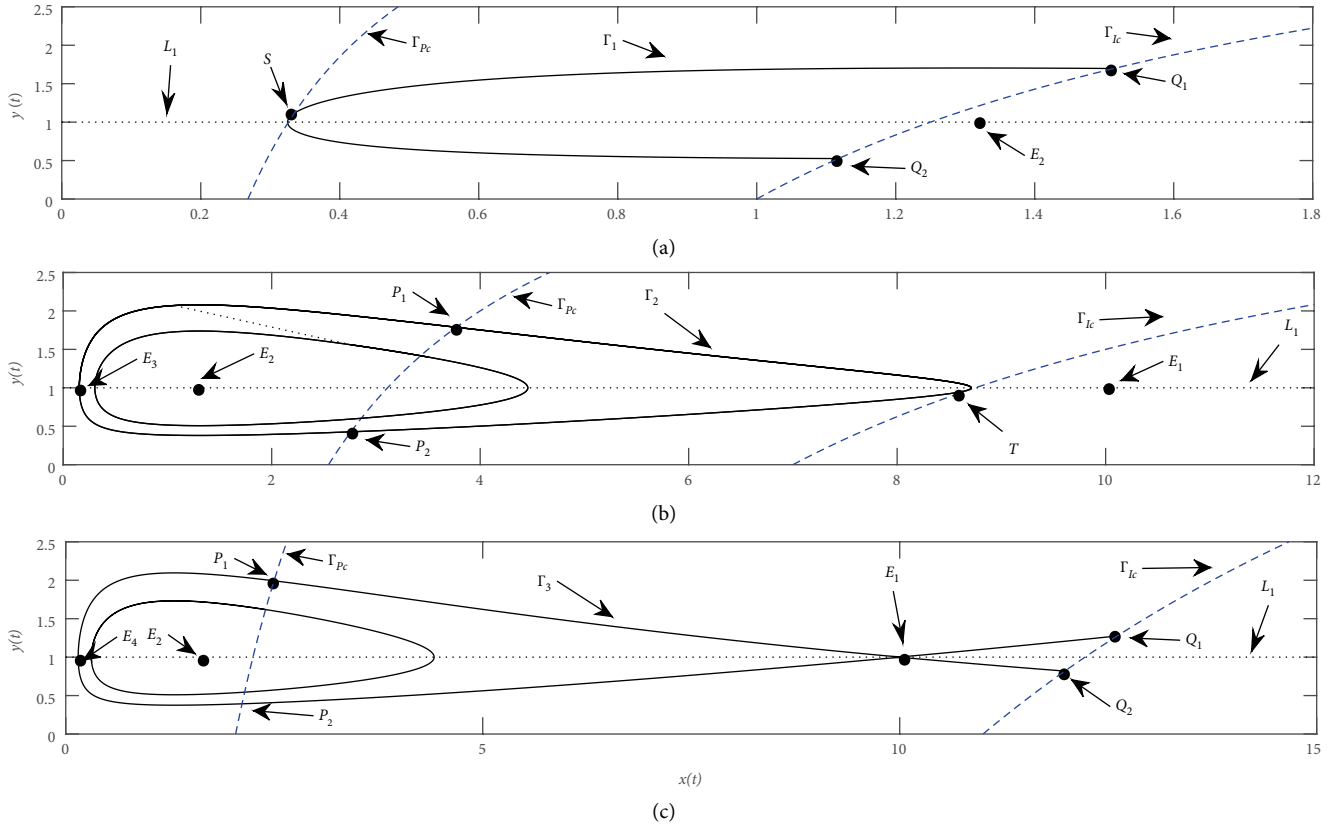

FIGURE 1: Illustration diagrams of the impulsive and phase sets for Cases (B_1), (B_2) and (B_3). (a) $AT/\alpha \le x_2^*$, (b) $x_2^* < (AT/\alpha) < x_1^*$, and (c) $AT/\alpha \ge x_1^*$. Γ_1 is a trajectory tangent to curve Γ_{Pc} at point $S = (x_S, y_S)$, Γ_2 is a trajectory tangent to curve Γ_{Ic} at point $T = (x_T, y_T)$, Γ_3 is homoclinic trajectory which touches curve Γ_{Pc} at two points (x_{P_1}, y_{P_1}) and (x_{P_2}, y_{P_2}), and its upper and lower right branches touch curve Γ_{Ic} at points $Q_1 = (x_{Q_1}, y_{Q_1})$ and $Q_2 = (x_{Q_2}, y_{Q_2})$, respectively.

management cost and the growth rules of the pest. Impulsive differential equations with impulses happening at fixed time emerge in the modelling of real-world phenomena in which the state of the inspected procedure fluctuates at fixed moments of time. In literature [30], the author extended a model with linear impulsive control tactics to a model with nonlinear impulsive control measures, which revealed further precise conditions for pest control. Wang et al. [31] discussed the threshold condition which guarantee the existence and stability criteria for the pest-free periodic solution. In addition, the complex dynamics for system is discussed when the forward and backward bifurcations could happen once the pest-free periodic solution becomes unstable.

State-dependent feedback control approach is generally expressed by an impulsive semi dynamical system, and they can be portrayed in comprehensive terms in real biological problems. For example, control tactics (i.e., pesticide application, harvesting, treatment, etc.) are applied only when a particular species size ranges an earlier known threshold density. Specifically, in [32–35] an excellent example in the series of models encouraged by IPM has been framed and examined. In [36–38], IPM has been exhibited by experiments, and it is demonstrated that IPM is more effective than classical methods.

In all the previous literatures, researchers projected models either with a single economic threshold or multiple thresholds [39–45]. There are few drawbacks to this sort of thresholds. However, there are two reasonable circumstances: one is that the number of the pest population is comparatively large, but its change rate is quite small; the other is that the number of population is small, but its change rate is significantly high. The latter case is more obvious at the initial stage of the occurrence of the pest. To overcome these drawbacks, we planned to take the model with action threshold depending on the pest density and its change rate (so-called ratio-dependent AT), and investigate its global dynamics.

The paper is ordered as follows: In Section 2, the commonly used generalized prey-predator model is proposed and the new ratio-dependent nonlinear action threshold is introduced. In Section 3, the exact impulsive and phase sets are determined for all existing cases. In view of the impulsive and phase sets, the Poincaré map is constructed in Section 4. In Section 5.1, some important relations and lemmas are provided that are very important for the next sections. The boundary order-1 periodic solution is given in Section 5.2. In Section 6, the global properties of system constructed in Section 2 are discussed, including the existence, local and global stability of order-1 periodic solution, and the effect of

weighted parameters on the fixed point of Poincaré map. In the same section, the effect of weighted parameters on the different cases is also discussed. To sum up the whole work, a detailed conclusion is given in Section 7.

2. Construction of Model and Main Properties

In view of the reasons specified above, we consider the commonly used prey-predator system with pest density and its change rate dependent feedback control, i.e., the action threshold depends not only on pest density but also on its change rate, which can be modeled by

$$\left.\begin{cases} \frac{dx(t)}{dt} = ax(t)\left(1-\frac{x(t)}{K}\right) - bx(t) - qx(t)y(t), \\ \frac{dy(t)}{dt} = \frac{\lambda x(t)y(t)}{1+wx(t)} - rx(t)y(t) - \delta y(t), \\ x(t^+) = (1-p)x(t), \\ y(t^+) = y(t)+\tau, \end{cases}\right\} \begin{matrix} \alpha x(t) + \beta\frac{dx(t)}{dt} < AT, \\ \alpha x(t) + \beta\frac{dx(t)}{dt} = AT, \end{matrix} \tag{1}$$

where α, β, and AT are all positive constants with $\alpha + \beta = 1$. $x(t)$ and y(t) respectively, represent the quantities of prey and predator. a denotes the intrinsic growth rate of the pest population and K demonstrates the carrying capacity. The pest population dies at the rate of $bx(t)$ and is predated by the predator population at a rate $qx(t)y(t)$. The quantity $(\lambda x(t)y(t))/(1+wx(t))$, which is actually a saturating function of the present quantity of pest, is the expand rate of predator response. The prey population breakdowns the predator response at a rate $rx(t)y(t)$, and $\delta y(t)$ represents the decay rate of the predator in the absence of prey. The quantities $(1-p)x(t)$ and $y(t)+\tau$ are known as the controlling quantities; whenever the pest population touches the action threshold, the management activities are adapted and the quantities of prey and predator are adjusted according to the controlling actions $(1-p)x(t)$ and $y(t)+\tau$ respectively. Therefore p denotes the instant killing rate and τ represents the releasing constant.

If the value of carrying capacity $K \to +\infty$, then for $c = a - b$ model (1) is reduced to the following form

$$\left.\begin{cases} \frac{dx(t)}{dt} = cx(t) - qx(t)y(t), \\ \frac{dy(t)}{dt} = \frac{\lambda x(t)y(t)}{1+wx(t)} - rx(t)y(t) - \delta y(t), \\ x(t^+) = (1-p)x(t), \\ y(t^+) = y(t)+\tau, \end{cases}\right\} \begin{matrix} \alpha x(t) + \beta\frac{dx(t)}{dt} < AT, \\ \alpha x(t) + \beta\frac{dx(t)}{dt} = AT. \end{matrix} \tag{2}$$

The quantities α and β are dependent weighted parameters. It is interesting to note that if the second weighted parameter β disappears, the ratio-dependent AT will transform into ET [41–45]. Therefore, the ET is an exceptional case of ratio-dependent AT for $\beta = 0$. From ratio-dependent AT and the first equation of model (2), it follows that $y = ((\alpha + c\beta)x - AT)/(q\beta x)$ with

$$\lim_{x\to+\infty} \frac{(\alpha+c\beta)x - AT}{q\beta x} = \frac{\alpha+c\beta}{q\beta}. \tag{3}$$

If the weighted parameter α vanishes, the ratio-dependent AT transformed into $y = (cx - AT)/(qx)$. It is obvious that if again pest population x tends to infinity, the predator population y is bounded and approaches its maximum value c/q. By applying the controlling quantities on $y = ((\alpha + c\beta)x - AT)/(q\beta x)$, we get another curve $y^+ = ((\alpha + c\beta)x^+ - AT(1-p))/(q\beta x^+) + \tau$. For $\beta = 0$, the curve transforms into the vertical straight line $x^+ = (1-p)AT$.

For convenience, we denote $y = ((\alpha + c\beta)x - AT)/(q\beta x)$ and $y^+ = (((\alpha + c\beta)x^+ - AT(1-p))/(q\beta x^+)) + \tau$ by Γ_{Ic} and Γ_{Pc} respectively, as shown in Figure 1. $(AT)/(\alpha + c\beta)$ is the initial value which curve Γ_{Ic} attains at $y = 0$. At this point, the vertical coordinate with Γ_{Pc} takes the value $(p(\alpha + c\beta))/(q\beta) + \tau$. If β approaches one, then x approaches $(AT)/c$ and hence in this case, the vertical coordinate with Γ_{Pc} attains the value $(pc/q) + \tau$. It is an essential assumption that the initial value x_0^+ must satisfy $\alpha x_0^+ + \beta(dx_0^+/dt) < AT$.

Our main objective is to discuss the global dynamics of model (2). We will see how the global dynamics are affected if the threshold is not a straight line but complex curve. For the first two equations (i.e., the ODE system without control measures), there always exist trivial equilibrium (0, 0) and two interior equilibria

$$E_1 = \left(x_1^*, \frac{c}{q}\right) \quad \text{and} \quad E_2 = \left(x_2^*, \frac{c}{q}\right), \tag{4}$$

where

$$x_1^* = \frac{\lambda - r - \delta\omega + \sqrt{(\lambda - r - \delta\omega)^2 - 4r\omega\delta}}{2r\omega} \tag{5}$$

and

$$x_2^* = \frac{\lambda - r - \delta\omega - \sqrt{(\lambda - r - \delta\omega)^2 - 4r\omega\delta}}{2r\omega} \tag{6}$$

provided that $\lambda - r - \delta\omega > 0$ and $\lambda - r - \delta\omega > 2\sqrt{r\delta\omega}$. If $\lambda - r - \delta\omega = 2\sqrt{r\delta\omega}$, then the two roots will coincide with each other. It is also clear that E_2 is the centre and E_1 is a saddle point.

Recently, Tang et al. [46] presented the following prey-predator model with state-dependent feedback control which is the special case of model (1) for $\alpha = 1$ and $\beta = 0$

$$\left.\begin{cases} \frac{dx(t)}{dt} = ax(t)\left(1-\frac{x(t)}{K}\right) - bx(t) - qx(t)y(t), \\ \frac{dy(t)}{dt} = \frac{\lambda x(t)y(t)}{1+wx(t)} - rx(t)y(t) - \delta y(t), \\ x(t^+) = (1-p)x(t), \\ y(t^+) = y(t)+\tau, \end{cases}\right\} \begin{matrix} x(t) < AT, \\ x(t) = AT, \end{matrix} \tag{7}$$

where AT signifies the economic threshold level, i.e., action threshold transforms into ET.

The special case of model (2) for $\omega = 0$ and $\lambda - r = d$ is

$$\left.\begin{cases} \frac{dx(t)}{dt} = cx(t) - qx(t)y(t), \\ \frac{dy(t)}{dt} = dx(t)y(t) - \delta y(t), \\ x(t^+) = (1-p)x(t), \\ y(t^+) = y(t)+\tau, \end{cases}\right\} \begin{matrix} \alpha x(t) + \beta\frac{dx(t)}{dt} < AT, \\ \alpha x(t) + \beta\frac{dx(t)}{dt} = AT, \end{matrix} \tag{8}$$

which has been considered in [47]. We will see that the results associated to model (8) can be easily obtained based on the results for model (2).

3. Impulsive and Phase Sets

In this section, we will find out the exact impulsive and phase sets for the existing cases. The foremost and necessary part is to search out the segment that is free from impulsive effect, i.e., the solution starting from Γ_{Pc} cannot reach to curve Γ_{Ic} for maximum impulsive set. Based on the positions of equilibria E_1, E_2 and curve Γ_{Ic}, we take the following three cases:

$$(B_1)\ \frac{AT}{\alpha} \le x_2^*;\quad (B_2)\ x_2^* < \frac{AT}{\alpha} < x_1^*\ \text{ and }\ (B_3)\ \frac{AT}{\alpha} \ge x_1^*. \tag{9}$$

3.1. Impulsive Set. In Case (B_1), trajectory Γ_1 is tangent to curve Γ_{Pc} at point $S = (x_S, y_S)$ with $y_S \ge c/q$. If we represent point $\left(x_{Q_2}, y_{Q_2}\right)$ by $\left(x_{im}^1, y_{im}^1\right)$, then the domain of the impulsive set becomes as:

$$\mathscr{M}_1 = \left\{(x,y) \in R_+^2 \middle| \frac{AT}{\alpha + c\beta} \le x \le x_{im}^1,\quad 0 \le y \le y_{im}^1\right\}. \tag{10}$$

It is obvious from the domain of impulsive set $\mathscr{M}_1$ that in this case, no solution originating from the phase set will reach the interval $\left(y_{im}^1, c/q\right]$. In the following lemma, we find out the exact value of y_{im}^1 which depends on the corresponding horizontal coordinate.

Lemma 1. *For Case (B_1), the impulsive set is defined as $\mathscr{M}_1$. The maximum vertical coordinate of $\mathscr{M}_1$ is y_{im}^1, where $y_{im}^1 = -(c/q)W\left(-(q/c)y_S e^{-(q/c)y_S + \left(A_{Q_2}^1/c\right)}\right)$ provided that $A_{Q_2}^1 \le 0$.*

Proof. Let a solution Γ_1 is tangent to curve Γ_{Pc} at point (x_S, y_S), and it touches curve Γ_{Ic} at point $Q_2 = \left(x_{Q_2}, y_{Q_2}\right)$. Then these points must satisfy the following equation

$$\frac{\lambda}{\omega}\ln\frac{1+\omega x_{Q_2}}{1+\omega x_S} - r\left(x_{Q_2} - x_S\right) - \delta\ \ln\frac{x_{Q_2}}{x_S} = c\ln\frac{y_{Q_2}}{y_S} - q\left(y_{Q_2} - y_S\right). \tag{11}$$

Solving this equation for y_{Q_2}, we get

$$\left(-\frac{q}{c}y_{Q_2}\right)e^{-(q/c)y_{Q_2}} = -\frac{q}{c}y_S e^{-(q/c)y_S + A_{Q_2}^1/c}, \tag{12}$$

where $A_{Q_2}^1 = (\lambda/\omega)\ln\left(\left(1+\omega x_{Q_2}\right)/\left(1+\omega x_S\right)\right) - r\left(x_{Q_2} - x_S\right) - \delta\ln\left(x_{Q_2}\right)/(x_S)$. We can solve the above equation with the help of Lambert W function. Obviously, the above equation will give us two solutions, but only the minimum value lies on curve Γ_{Ic} as well as Γ_1. If we denote it by y_{im}^1, we obtain

$$y_{im}^1 = -\frac{c}{q}W\left(-\frac{q}{c}y_S e^{-(q/c)y_S + A_{Q_2}^1/c}\right), \tag{13}$$

which is well defined due to $A_{Q_2}^1 \le 0$.

From Figure 1(b), it can be seen that for Case (B_2), Γ_2 is tangent to curve Γ_{Ic} at point $T = (x_T, y_T)$, where $y_T \le (c/q)$. Then based on the positions of equilibria E_1, E_2 and curve Γ_{Ic}, we discuss the maximum impulsive set for this case as follows:

$$\mathscr{M}_2 = \left\{(x,y) \in R^2 \middle| \frac{AT}{\alpha + c\beta} \le x \le x_T,\quad 0 \le y \le y_T\right\}. \tag{14}$$

The tangent point of the closed trajectory with curve Γ_{Ic} varies with the changing estimations of weighted parameters α and β. From the domain of impulsive set $\mathscr{M}_2$, it is obvious that if $y_T < c/q$ then the interval $\left(y_T, (c/q)\right]$ cannot be used for any solution originating from the respective phase set.

Now we discuss the impulsive set for the Case (B_3). This case is more crucial than the previous cases. In this case, homoclinic trajectory exists. This homoclinic trajectory Γ_3 touches curve Γ_{Pc} at points $\left(x_{P_1}, y_{P_1}\right)$ and $\left(x_{P_2}, y_{P_2}\right)$, and its lower right branch touches curve Γ_{Ic} at point $Q_2 = \left(x_{Q_2}, y_{Q_2}\right)$ (as shown in Figure 1(c)). This is actually the maximum impulsive point for Case (B_3). Before finding out the exact value of vertical coordinate y_{Q_2}, we first provide some necessary quantities which are not only helpful for finding the maximum vertical coordinate of the impulsive set $\mathscr{M}_3$, but also assume a significant role in finding the fixed point of the Poincaré map $P\left(y_i^+\right)$. These quantities are listed as follows:

$$A_{P_1}^3 = \frac{\lambda}{\omega}\ln\frac{1+\omega x_1^*}{1+\omega x_{P_1}} - r\left(x_1^* - x_{P_1}\right) - \delta\ \ln\frac{x_1^*}{x_{P_1}}, \tag{15}$$

$$A_1 = \frac{\lambda}{\omega}\ \ln\frac{1+\omega x_{Q_2}}{1+\omega x_{P_1}} - r\left(x_{Q_2} - x_{P_1}\right) - \delta\ \ln\frac{x_{Q_2}}{x_{P_1}}, \tag{16}$$

$$A_{Q_2}^3 = A_{P_1}^3 - A_1 = \frac{\lambda}{\omega}\ln\frac{1+\omega x_1^*}{1+\omega x_{Q_2}} - r\left(x_1^* - x_{Q_2}\right) - \delta\ln\frac{x_1^*}{x_{Q_2}}. \tag{17}$$

Replacing x_{P_1} by x_{P_2} in equations (15) and (16) and denoting the resultant equations by $A_{P_2}^3$ and A_2 respectively, then $A_{Q_2}^3 = A_{P_2}^3 - A_2$. If we denote $\left(x_{Q_2}, y_{Q_2}\right)$ by $\left(x_{im}^3, y_{im}^3\right)$, then we find the exact value of y_{im}^3 which depends on the respective horizontal coordinate. □

Lemma 2. *For Case (B_3), the impulsive set is defined as $\mathscr{M}_3$. The maximum vertical coordinate for this is y_{im}^3, where $y_{im}^3 = -(c/q)W\left(-e^{-1-\left(A_{Q_2}^3/c\right)}\right)$ provided that $A_{Q_2}^3 \ge 0$.*

Proof. In this case, the lower right branch of the homoclinic trajectory Γ_3 touches curve Γ_{Ic} at point $Q_2 = \left(x_{Q_2}, y_{Q_2}\right)$. Combining point $Q_2 = \left(x_{Q_2}, y_{Q_2}\right)$ with $E_1 = \left(x_1^*, c/q\right)$ must satisfy the following relation:

$$\begin{aligned} c\ln\frac{c}{q} - c - \frac{\lambda}{\omega}\ln\left(1+\omega x_1^*\right) + r x_1^* + \delta\ln x_1^* &= c\ln y_{Q_2} - q y_{Q_2} \\ &- \frac{\lambda}{\omega}\ln\left(1+\omega x_{Q_2}\right) + r x_{Q_2} + \delta\ln x_{Q_2}, \end{aligned} \tag{18}$$

which can be simplified as

$$\frac{\lambda}{\omega}\ln\frac{1+\omega x_1^*}{1+\omega x_{Q_2}} - r\left(x_1^* - x_{Q_2}\right) - \delta\ln\frac{x_1^*}{x_{Q_2}} = c\ln\frac{c/q}{y_{Q_2}} - q\left(\frac{c}{q} - y_{Q_2}\right). \tag{19}$$

Solving the above equation for y_{Q_2}, we get

$$\left(-\frac{q}{c}y_{Q_2}\right)e^{-(q/c)y_{Q_2}} = -e^{-1-A^3_{Q_2}/c}. \tag{20}$$

Following the same way as in Lemma 1, applying the properties of Lambert W function, we get two solutions. From Figure 1(c) it is clear that only the minimum value lies both on curve Γ_3 and Γ_{Ic}. If we denote it by y^3_{im}, then we get

$$y^3_{im} = -\frac{c}{q}W\left(-e^{-1-A^3_{Q_2}/c}\right), \tag{21}$$

which is well defined due to $A^3_{Q_2} \geq 0$. If we represent the impulsive set by $\mathscr{M}_3$, then it can be expressed as

$$\mathscr{M}_3 = \left\{(x, y) \in R^2 \middle| \frac{AT}{\alpha + c\beta} \leq x \leq x^3_{im}, \quad 0 \leq y \leq y^3_{im}\right\}. \tag{22}$$

3.2. Phase Set. In this subsection, we aim to discuss the phase sets for all the existing cases expressed above. The most essential and tough task in the process of discussing phase sets is to find out the segment, which is free from the impulsive effect. To find the exact domain of phase sets, we provide the following intervals:

$$X^1_D = \left[\frac{AT(1-p)}{\alpha + c\beta}, (1-p)x^1_{im}\right], \; Y^1_D = \left[\tau, y^1_{im} + \tau\right],$$
$$X^2_D = \left[\frac{AT(1-p)}{\alpha + c\beta}, (1-p)x_T\right], \tag{23}$$

$$Y^2_D = [\tau, y_T + \tau], \; X^3_D = \left[\frac{AT(1-p)}{\alpha + c\beta}, (1-p)x^3_{im}\right], \text{ and } Y^3_D = \left[\tau, y^3_{im} + \tau\right]. \tag{24}$$

For Case (B_1), trajectory Γ_1 is tangent to curve Γ_{Pc} at point $S = (x_S, y_S)$. Thus, the corresponding phase set to the impulsive set $\mathscr{M}_1$ can be expressed as:

$$\mathscr{N}_1 = \left\{(x^+, y^+) \in R^2_+ \middle| x^+ \in X^1_D, y^+ \in Y^1_D\right\} \tag{25}$$

For Case (B_2), the closed trajectory is tangent to curve Γ_{Ic} at point $T = (x_T, y_T)$, where $y_T \leq (c/q)$. We indicate the intersection point of the closed trajectory Γ_2 with line $y = c/q$ (denoted by L_1) as $E_3 = (x_3, y_3)$. If we denote $\left(x_{P_2}, y_{P_2}\right)$ by $\left(x^2_{\min}, y^2_{\min}\right)$ and $\left(x_{P_1}, y_{P_1}\right)$ by $\left(x^2_{\max}, y^2_{\max}\right)$, then the phase set corresponds to the impulsive set $\mathscr{M}_2$ can be expressed as follows:

$$\mathscr{N}_2 = \left\{(x^+, y^+) \in R^2_+ \middle| \, x^+ \in X^2_{Ps}, y^+ \in Y^2_{Ps}\right\} \tag{26}$$

with

$$X^2_{Ps} = \left\{\left[\frac{AT(1-p)}{\alpha + c\beta + \tau q\beta}, x^2_{\min}\right] \cup \left[x^2_{\max}, +\infty\right)\right\} \cap X^2_D \tag{27}$$

and

$$Y^2_{Ps} = \left\{\left[0, y^2_{\min}\right] \cup \left[y^2_{\max}, \frac{(\alpha + c\beta)}{q\beta} + \tau\right)\right\} \cap Y^2_D. \tag{28}$$

From the phase set $\mathscr{N}_2$, it is clear that the solution initiating from the interval $\left(y^2_{\min}, y^2_{\max}\right)$ will be free from impulsive effect. In the following lemma, based on the respective horizontal coordinates, the exact values of $y^2_{\max}$ and $y^2_{\min}$ are given.

Lemma 3. *For Case (B_2), the impulsive set is defined as $\mathscr{M}_2$. In this case, any solution initiating from $\left(y^2_{\min}, y^2_{\max}\right)$ will be free from impulse effect, where*

$$y^2_{\max} = -\frac{c}{q}W\left(-1, -\frac{q}{c}y_T e^{-(q/c)y_T - A^2_{P_1}/c}\right) \; \textit{and}$$
$$y^2_{\min} = -\frac{c}{q}W\left(-\frac{q}{c}y_T e^{-(q/c)y_T - A^2_{P_2}/c}\right) \tag{29}$$

provided that $A^2_{P_1}, A^2_{P_2} \geq 0$.

Proof. Suppose that the closed trajectory Γ_2 originates from $\left(x_{P_1}, y_{P_1}\right)$, and tangent to curve Γ_{Ic} at point (x_T, y_T). Then, these points must satisfy the relation:

$$\frac{\lambda}{\omega}\ln\frac{1+\omega x_T}{1+\omega x_{P_1}} - r\left(x_T - x_{P_1}\right) - \delta \ln\frac{x_T}{x_{P_1}} = c \ln\frac{y_T}{y_{P_1}} - q\left(y_T - y_{P_1}\right). \tag{30}$$

Rearranging this equation for y_{P_1}, we get

$$\left(-\frac{q}{c}y_{P_1}\right)e^{-(q/c)y_{P_1}} = -\frac{q}{c}y_T e^{-(q/c)y_T - A^2_{P_1}/c}, \tag{31}$$

where $A^2_{P_1} = \left((\lambda/\omega)\ln(1+\omega x_T)/\left(1+\omega x_{P_1}\right)\right) - r\left(x_T - x_{P_1}\right) - \delta \ln\left(x_T/x_{P_1}\right)$. The above equation can be solved with the help of Lambert W function. If we denote the maximum solution by $y^2_{\max}$, we get

$$y^2_{\max} = -\frac{c}{q}W\left(-1, -\frac{q}{c}y_T e^{-(q/c)y_T - A^2_{P_1}/c}\right). \tag{32}$$

The value of y_{P_2}, denoted by $y^2_{\min}$ can also be found by using the same method as above, i.e.,

$$y^2_{\min} = -\frac{c}{q}W\left(-\frac{q}{c}y_T e^{-(q/c)y_T - A^2_{P_2}/c}\right) \tag{33}$$

with $A^2_{P_2} = (\lambda/\omega)\ln\left(\left(1+\omega x_T\right)/\left(1+\omega x_{P_2}\right)\right) - r\left(x_T - x_{P_2}\right) - \delta \ln\left(x_T/x_{P_2}\right)$.

If weighted parameter $\beta = 0$, i.e., the threshold level only depends on the pest density then the closed trajectory becomes tangent at $y = c/q$. In this case, $y^2_{\min}$ and $y^2_{\max}$ become as

$$y^2_{\max} = -\frac{c}{q}W\left(-1, -e^{-1-A^2_P/c}\right), \text{ and } y^2_{\min} = -\frac{c}{q}W\left(-e^{-1-A^2_P/c}\right) \tag{34}$$

with $A^2_{P_1} = A^2_{P_2} = A^2_P$.

For Case (B_3), let us denote the intersection of the homoclinic trajectory Γ_3 with line $y = c/q$ (denoted by L_1) as $E_4 = (x_4, y_4)$. Trajectory Γ_3 touches curve Γ_{Pc} at upper point $P_1 = \left(x_{P_1}, y_{P_1}\right)$ and lower point $P_2 = \left(x_{P_2}, y_{P_2}\right)$, denoted by $\left(x^3_{\max}, y^3_{\max}\right)$ and $\left(x^3_{\min}, y^3_{\min}\right)$ respectively. In the following lemma, we find the exact values of $y^3_{\max}$ and $y^3_{\min}$.

Lemma 4. *For Case (B_3), the impulsive set is defined as $\mathscr{M}_3$. In this case any solution initiating from $\left[y^3_{\min}, y^3_{\max}\right]$ will be free from impulse effect, where*

$$y^3_{\max} = -\frac{c}{q}W\left(-1, -e^{-1-A^3_{P_1}/c}\right) \text{ and } y^3_{\min} = -\frac{c}{q}W\left(-e^{-1-A^3_{P_2}/c}\right) \tag{35}$$

provided that $A^3_{P_1}, A^3_{P_2} \geq 0$.

Proof. Suppose that the homoclinic trajectory Γ_3 touches curve Γ_{Pc} at upper point $P_1 = \left(x_{P_1}, y_{P_1}\right)$. Combining point $P_1 = \left(x_{P_1}, y_{P_1}\right)$ with $E_1 = \left(x^*_1, (c/q)\right)$ must satisfy the following relation:

$$\frac{\lambda}{\omega}\ln\frac{1+\omega x^*_1}{1+\omega x_{P_1}} - r\left(x^*_1 - x_{P_1}\right) - \delta\ln\frac{x^*_1}{x_{P_1}} = c\ln\frac{c/q}{y_{P_1}} - q\left(\frac{c}{q} - y_{P_1}\right). \tag{36}$$

Arranging this equation for y_{P_1}, we get

$$\left(-\frac{q}{c}y_{P_1}\right)e^{-(q/c)y_{P_1}} = -e^{-1-A^3_{P_1}/c}, \tag{37}$$

where $A^3_{P_1} = (\lambda/\omega)\ln\left((1+\omega x^*_1)/\left(1+\omega x_{P_1}\right)\right) - r\left(x^*_1 - x_{P_1}\right) - \delta\ln\left(x^*_1\right)/\left(x_{P_1}\right)$. The above equation can be solved with the help of Lambert W function. If we denote the maximum solution by $y^3_{\max}$, we get

$$y^3_{\max} = -\frac{c}{q}W\left(-1, -e^{-1-A^3_{P_1}/c}\right). \tag{38}$$

The value of y_{P_2}, denoted by $y^3_{\min}$ can also be found by following the same way as above, i.e.,

$$y^3_{\min} = -\frac{c}{q}W\left(-e^{-1-A^3_{P_2}/c}\right) \tag{39}$$

with $A^3_{P_2} = (\lambda/\omega)\ln\left((1+\omega x^*_1)/\left(1+\omega x_{P_2}\right) - r\left(x^*_1 - x_{P_2}\right)\right) - \delta\ln\left(x^*_1/x_{P_2}\right)$.

If we represent the phase set for Case (B_3) by $\mathscr{N}_3$, then it can be expressed as

$$\mathscr{N}_3 = \left\{\left(x^+, y^+\right) \in R^2_+ \middle| x^+ \in X^3_{Ps}, y^+ \in Y^3_{Ps}\right\} \tag{40}$$

with

$$X^3_{Ps} = \left\{\left[\frac{AT(1-p)}{\alpha + c\beta + \tau q\beta}, x^3_{\min}\right) \cup \left(x^3_{\max}, +\infty\right)\right\} \cap X^3_D \tag{41}$$

and

$$Y^3_{Ps} = \left\{\left[0, y^3_{\min}\right) \cup \left(y^3_{\max}, \frac{(\alpha + c\beta)}{q\beta} + \tau\right)\right\} \cap Y^3_D. \tag{42}$$

If Γ_{Pc} lies on the left and does not touch Γ_2 or Γ_3, then the impulsive and phase sets will be transformed into $\mathcal{M}_1$ and $\mathcal{N}_1$, respectively.

3.3. The Impulsive and Phase Sets for Model (8). In view of the model (2) and based on the locations of curve Γ_{Ic} and stable center $(\delta/d, c/q)$, the following two cases can be taken for model (8)

$$\left(B^0_1\right) \ \frac{AT}{\alpha} \leq \frac{\delta}{d} \text{ and } \left(B^0_2\right) \ \frac{\delta}{d} < \frac{AT}{\alpha}. \tag{43}$$

In the first case, trajectory Γ^0_1 is tangent to curve Γ_{Pc} at point $S_0 = \left(x_{S_0}, y_{S_0}\right)$ with $y_{S_0} \geq c/q$ (as shown in Figure 2(a)). If we represent point $\left(x_{Q_2}, y_{Q_2}\right)$ by $\left(x^0_{im}, y^0_{im}\right)$, then the impulsive set $\mathscr{M}^0_1$ can be expressed as

$$\mathscr{M}^0_1 = \left\{(x, y) \in R^2_+ \middle| \frac{AT}{\alpha + c\beta} \leq x \leq x^0_{im}, \quad 0 \leq y \leq y^0_{im}\right\}. \tag{44}$$

To discuss the exact domains of the phase set for both cases, we define the intervals $X^1_{D_0} = \left[(AT(1-p))/(\alpha + c\beta), (1-p)x^0_{im}\right], Y^1_{D_0} = \left[\tau, y^0_{im} + \tau\right], X^2_{D_0} = \left[(AT(1-p))/(\alpha + c\beta), \left(1-p\right)x_{T_0}\right]$ and $Y^2_{D_0} = \left[\tau, y_{T_0} + \tau\right]$. Then, the phase set for Case $\left(B^0_1\right)$ becomes as:

$$\mathcal{N}^0_1 = \left\{\left(x^+, y^+\right) \in R^2_+ \middle| x^+ \in X^1_{D_0}, y^+ \in Y^1_{D_0}\right\} \tag{45}$$

In the following lines the analytical value of y^0_{im} is given. The proof of the lemma is the same as previous section, so we omit it. □

Lemma 5. *For Case $\left(B^0_1\right)$, the impulsive set is defined as $\mathscr{M}^0_1$. The maximum vertical coordinate for this is y^0_{im}, where $y^0_{im} = -(c/q)W\left(-(q/c)y_{S_0}e^{-(q/c)y_{S_0} + \left(A_{Q_2}/c\right)}\right)$ provided that $A_{Q_2} = \delta\left(\ln x_{S_0} - \ln x_{Q_2}\right) + d\left(x_{Q_2} - x_{S_0}\right) \leq 0$.*

For Case $\left(B^0_2\right)$, we denote the intersection point of the closed trajectory Γ^0_2 with line $y = c/q$ (denoted by L_1) as $E_1 = \left(x_{E_1}, y_{E_1}\right)$. In this case, the closed trajectory is tangent to curve Γ_{Ic} at point $T_0 = \left(x_{T_0}, y_{T_0}\right)$, where $y_{T_0} \leq c/q$. If we denote $\left(x_{P_2}, y_{P_2}\right)$ by $\left(x^0_{\min}, y^0_{\min}\right)$ and $\left(x_{P_1}, y_{P_1}\right)$ by $\left(x^0_{\max}, y^0_{\max}\right)$, then based on the positions of curves Γ_{Ic} and Γ_{Pc}, we discuss the impulsive and phase sets as follows:

$$\mathscr{M}^0_2 = \left\{(x, y) \in R^2 \middle| \frac{AT}{\alpha + c\beta} \leq x \leq x_{T_0}, \quad 0 \leq y \leq y_{T_0}\right\}, \tag{46}$$

$$\mathscr{N}^0_2 = \left\{\left(x^+, y^+\right) \in R^2_+ \middle| x^+ \in X^{02}_{Ps}, y^+ \in Y^{02}_{Ps}\right\} \tag{47}$$

with

$$X^{02}_{Ps} = \left\{\left[\frac{AT(1-p)}{\alpha + c\beta + \tau q\beta}, x^0_{\min}\right] \cup \left[x^0_{\max}, +\infty\right)\right\} \cap X^2_{D_0} \tag{48}$$

and

$$Y^{02}_{Ps} = \left\{\left[0, y^0_{\min}\right] \cup \left[y^0_{\max}, \frac{(\alpha + c\beta)}{q\beta} + \tau\right)\right\} \cap Y^2_{D_0}. \tag{49}$$

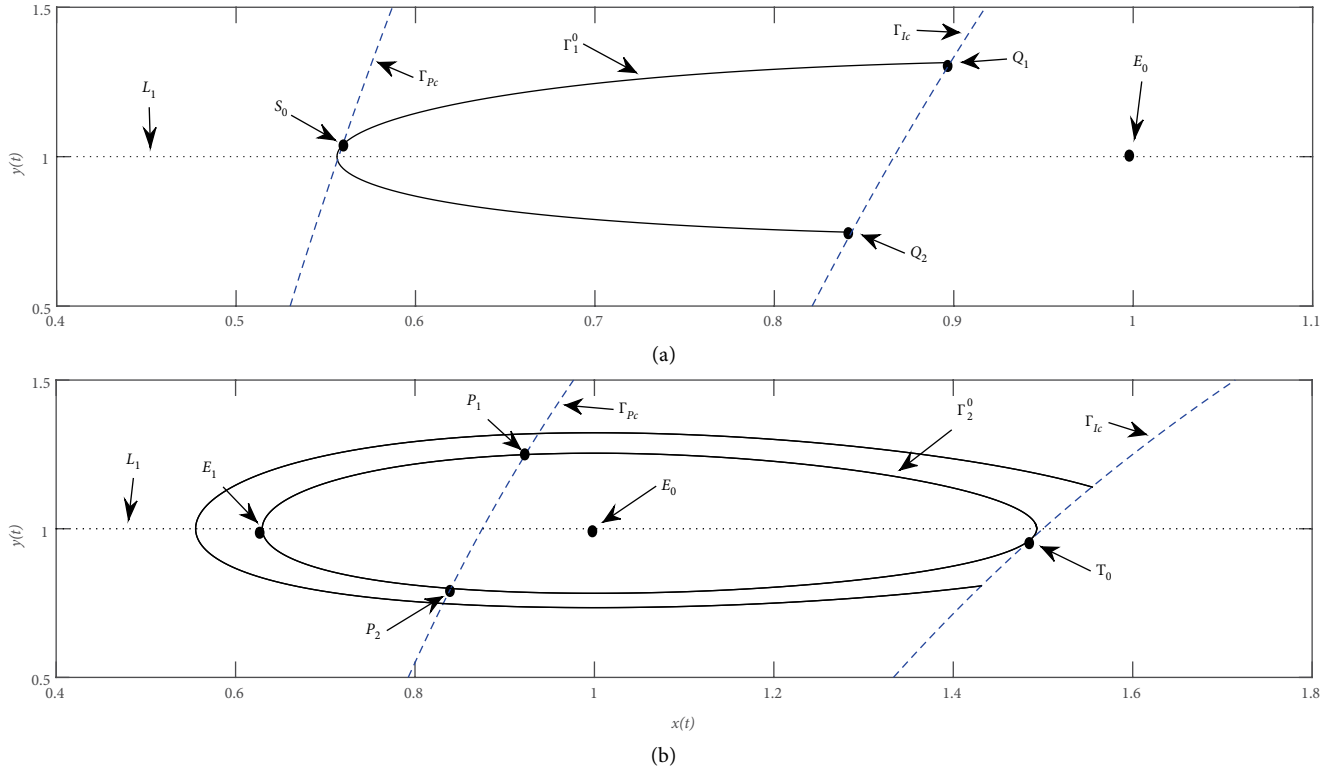

FIGURE 2: Illustration diagrams of the impulsive and phase sets for model (8). (a) $(AT/\alpha) \le (\delta/d)$, (b) $(\delta/d) < (AT/\alpha)$. Γ_1^0 is a trajectory tangent to curve Γ_{Pc} at point $S_0 = \left(x_{S_0}, y_{S_0}\right)$, and Γ_2^0 is a trajectory which is tangent to curve Γ_{Ic} at point $T_0 = \left(x_{T_0}, y_{T_0}\right)$.

From the phase set, it is clear that the solution initiating from the interval $\left(y^0_{\min}, y^0_{\max}\right)$ will be free from impulsive effect.

Lemma 6. *For Case $\left(B_2^0\right)$, the impulsive set is defined as $\mathscr{M}_2^0$. In this case any solution initiating from $\left(y^0_{\min}, y^0_{\max}\right)$ will be free from impulse effect, where*

$$y^0_{\max} = -\frac{c}{q}W\left(-1, -\frac{q}{c}y_{T_0}e^{-(q/c)y_{T_0}-A_{P_1}/c}\right) \quad \text{and}$$
$$y^0_{\min} = -\frac{c}{q}W\left(-\frac{q}{c}y_{T_0}e^{-(q/c)y_{T_0}-A_{P_2}/c}\right) \tag{50}$$

provided that

$$A_{P_1} = \delta\left(\ln x_{P_1} - \ln x_{T_0}\right) + d\left(x_{T_0} - x_{P_1}\right) \ge 0,$$
$$A_{P_2} = \delta\left(\ln x_{P_2} - \ln x_{T_0}\right) + d\left(x_{T_0} - x_{P_2}\right) \ge 0. \tag{51}$$

The proof of the Lemma 6 can also be shown as previous section, so we also omit it. If the weighted parameter $\beta = 0$, i.e., the threshold level only depends on the pest density then the closed trajectory Γ_2^0 becomes tangent to curve Γ_{Ic} at $y = c/q$. In this case, $y^0_{\min}$ and $y^0_{\max}$ become as:

$$y^0_{\max} = -\frac{c}{q}W\left(-1, -e^{-1-A_P/c}\right), \quad y^0_{\min} = -\frac{c}{q}W\left(-e^{-1-A_P/c}\right), \tag{52}$$

with $A_{P_1} = A_{P_2} = A_P$.

Compared with published work for model (8), we can see that more accurate domains of the impulsive and phase sets have been provided here. From Figure 2(b), it is clear that $x_{E_1} < (AT(1-p))/(\alpha + \tau q\beta) < (\delta/d)$.

In the upcoming discussions, for convenience, we use A_l rather than $A^1_{Q_2}, A^2_{P_1}, A^2_{P_2}$ or A_1. For Case (B_1), $A^1_{Q_2} \le 0$ is equivalent to $A_l \le 0$. For Case (B_2), $A_l \ge 0 \Longleftrightarrow A^2_{P_1}, A^2_{P_2} \ge 0$ and to avoid the complexity, we will focus only on $A_l > 0$. Similarly, for Case (B_3) it will be more convenient to denote A_1 and A_2 by A_l, $A^3_{P_1}$ and $A^3_{P_2}$ by A_u, and $A^3_{Q_2}$ by A_v.

4. Formation of Poincaré Map

Theorem 1. *The Poincaré map for the impulsive points of model (2) can be defined as follows:*

$$B_1: \quad y^+_{i+1} = P\left(y^+_i\right), \quad y^+_i \in Y^1_D \quad if \quad A_l \le 0, \tag{53}$$

$$B_2: \quad y^+_{i+1} = P\left(y^+_i\right), \quad y^+_i \in Y^2_{Ps} \quad if \quad A_l > 0, \tag{54}$$

$$B_3: \quad y^+_{i+1} = P\left(y^+_i\right), \quad y^+_i \in Y^3_{Ps} \quad if \quad A_u \ge A_l < 0 \quad or \quad A_u \ge 0 \ge A_l, \tag{55}$$

where

$$y^+_{i+1} = -\frac{c}{q}W\left[-\frac{q}{c}y^+_i\left(\exp\left(-\frac{q}{c}y^+_i + \frac{A_l}{c}\right)\right)\right] + \tau = P\left(y^+_i\right). \tag{56}$$

Proof. Assume that a trajectory originate from $\left(x^+_0, y^+_0\right)$ and repeats the pulse action k times, which can be finite or infinite. Let $p^+_0 = \left(x^+_i, y^+_i\right) \in \Gamma_{Pc}$ and $p_1 = \left(x_{i+1}, y_{i+1}\right) \in \Gamma_{Ic}$ be two points of the same trajectory. Then for these points, the following relation can easily be obtained:

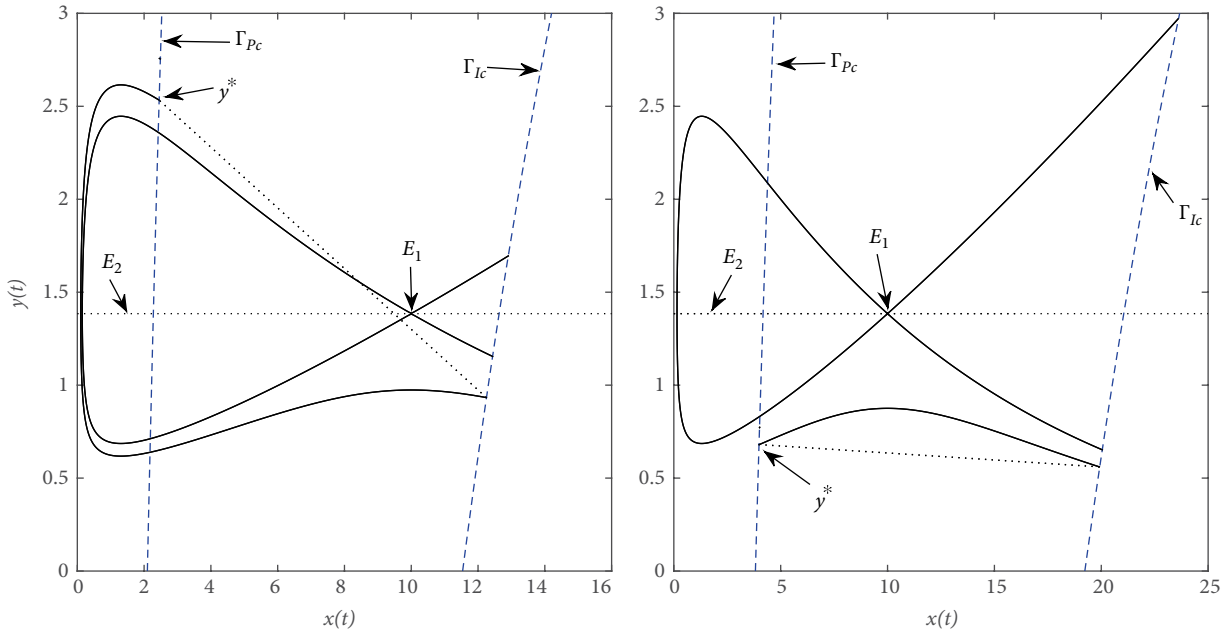

FIGURE 3: Fixed point of Poincaré map for Case (C_3). (a) $A_l = 0.2802$, $\tau = 1.6$, $\tau_3 = 1.2055$, $y^* = 2.5330$, $AT = 12$. (b) $A_l = -0.2054$, $\tau = 0.12$, $\tau_4 = 0.1801$, $y^* = 0.6798$, $AT = 20$. All other parameter values are fixed as: $\alpha = 0.95$, $\beta = 0.05$, $c = 1.8$, $q = 1.3$, $\lambda = 0.52$, $\omega = 0.1$, $r = 0.23$, $\delta = 0.3$, $p = 0.8$.

$$\frac{\lambda}{\omega}\ln\frac{1+\omega x_{i+1}}{1+\omega x_i^+} - r(x_{i+1} - x_i^+) - \delta\ln\frac{x_{i+1}}{x_i^+} = c\ln\frac{y_{i+1}}{y_i^+} - q(y_{i+1} - y_i^+). \tag{57}$$

Applying the properties of Lambert W function and solving the above equation for y_{i+1}, we get

$$y_{i+1} = -\frac{c}{q}W\left[-\frac{q}{c}y_i^+\left(\exp\left(-\frac{q}{c}y_i^+ + \frac{A_l}{c}\right)\right)\right], \tag{58}$$

where

$$A_l = \frac{\lambda}{\omega}\ln\frac{1+\omega x_{i+1}}{1+\omega x_i^+} - r(x_{i+1} - x_i^+) - \delta\ln\frac{x_{i+1}}{x_i^+}. \tag{59}$$

From (58), we get

$$y_{i+1}^+ = -\frac{c}{q}W\left[-\frac{q}{c}y_i^+\left(\exp\left(-\frac{q}{c}y_i^+ + \frac{A_l}{c}\right)\right)\right] + \tau = P(y_i^+). \tag{60}$$

Case (B_1): If $A_l \le 0$, then for $y_i^+ \ge 0$, equations (58) and (60) are well defined. Actually, if we define $g(y) = -(q/c)y\exp(-(q/c)y)$ then

$$g'(y) = \frac{q^2}{c^2}\exp\left(-\frac{q}{c}y\right)\left(y - \frac{c}{q}\right), \tag{61}$$

and it can easily be shown that $g(y)$ achieves its minimum value $-e^{-1}$ at point $y = c/q$. Therefore, $-(q/c)y\exp(-(q/c)y)\exp(A_l/c) \in [-e^{-1}, 0)$ for all $A_l \le 0$ and $y > 0$. This shows that the Poincaré map is defined by (53) for Case (B_1).

Now in order to demonstrate the exact domains of the Poincaré map for Cases (B_2) and (B_3), the most important part is to find the section of the phase set that is free from impulsive effect, i.e., the solution originating from $p_0^+ \in \Gamma_{Pc}$ cannot reach to point $p_1 \in \Gamma_{Ic}$.

Case (B_2): From Lemma 3, it is obvious that if the starting point $p_0^+ = (x_i^+, y_i^+)$ lies inside of the closed trajectory Γ_2, then trajectory cannot reach to curve Γ_{Ic}. This indicates that points p_0^+ and p_1 cannot lie in the same trajectory, as shown in Figure 1(b). From Lemma 3, it also follows that in this case, we have $A_l > 0$ and we need $p_0^+ \in \mathcal{N}_2$.

If $A_l > 0$, then $-(q/c)y\exp(-(q/c)y)\exp(A_l/c) \ge -e^{-1}$. From this, we get

$$\frac{q}{c}y\exp\left(-\frac{q}{c}y\right) \le \exp\left(-1 - \frac{A_l}{c}\right). \tag{62}$$

The solution gives $y \in (0, y_{\min}^2] \cup [y_{\max}^2, (\alpha + c\beta)/q\beta + \tau)$ and from Lemma 3 we know that

$$\begin{aligned} y_{\min}^2 &= -\frac{c}{q}W\left(-\frac{q}{c}y_T e^{-(q/c)y_T - A_{P_2}^2/c}\right) \text{ and} \\ y_{\max}^2 &= -\frac{c}{q}W\left(-1, -\frac{q}{c}y_T e^{-(q/c)y_T - A_{P_1}^2/c}\right), \end{aligned} \tag{63}$$

The Case (B_3) can be attained directly from the domains of the Poincaré map and applying the proof of Lemma 4. For this case $A_u \ge 0$, regardless of $A_l > 0$ or $A_l \le 0$ (as shown in Figure 3), the Poincaré map is given by the case (55). This completes the proof. □

Difference equation (56) which explains the Poincaré map reveals the relations between the impulsive points y_i^+ and y_{i+1}^+, so the existence and stability of fixed point of equation (56) indicate the existence and stability of order-1 periodic solution

of system (2). Therefore, we conclude that the properties of the Poincaré map play an essential role in exploring the impulsive semi-dynamical system.

Corollary 1. *The Poincaré map for model (8) can be defined as:*

$$y_{i+1}^{+} = \begin{cases} P(y_i^+), & y_i^+ \in Y_{D_0}^1 \text{ if } A_{Q_2} \le 0, \\ P(y_i^+), & y_i^+ \in Y_{Ps}^{02} \text{ if } A_{P_1}, A_{P_2} > 0. \end{cases} \tag{64}$$

Following the same way as in Theorem 1, we can show that the Poincaré map for model (8) is true. For convenience, we use A_l^0 rather than A_{Q_2} or A_{P_1} or A_{P_2}.

5. Characterization of Periodic Solution for $\tau = 0$

In this section, we will focus on the boundary order-1 periodic solution for system (2). To prove this, we first provide some significant relations and lemmas in the following subsection.

5.1. Some Important Relations and Notations. In view of the domains of the Poincaré map $P(y_i^+)$ characterized in Section 4 or the signs of A_l and A_u, we modify the Cases (B_1)–(B_3) as:

$$\begin{aligned} &(C_1)\ A_l \le 0;\ (C_2)\ A_l < 0 \ \text{ and} \\ &(C_3)\ (i)\ A_u \ge A_l < 0,\ (ii)\ A_u \ge 0, A_l \le 0. \end{aligned} \tag{65}$$

This shows that the sign of A_l is crucial for coming analysis. So, while choosing the parameters, we should be very careful. If we change the value of weighted parameters, the sign of A_l not necessarily remains the same.

The fixed point of the Poincaré map can be found directly from the analytical formula of the Poincaré map derived in Section 4. To do this, let

$$y^* = -\frac{c}{q} W\left[-\frac{q}{c} y^* \left(\exp\left(-\frac{q}{c} y^* + \frac{A_l}{c}\right)\right)\right] + \tau, \tag{66}$$

i.e.,

$$-\frac{q}{c}(y^* - \tau) = W\left[-\frac{q}{c} y^* \left(\exp\left(-\frac{q}{c} y^* + \frac{A_l}{c}\right)\right)\right]. \tag{67}$$

By applying the properties of Lambert W function, we get

$$-\frac{q}{c}(y^* - \tau)\exp\left(-\frac{q}{c}(y^* - \tau)\right) = -\frac{q}{c} y^* \exp\left(-\frac{q}{c} y^* + \frac{A_l}{c}\right), \tag{68}$$

This demonstrates that there exists a unique fixed point

$$y^* = \frac{\tau}{1 - \exp((A_l/c) - (q/c)\tau)} \tag{69}$$

or

$$y^* = \tau \frac{\exp((q/c)\tau - (A_l/c))}{\exp((q/c)\tau - (A_l/c)) - 1}. \tag{70}$$

Whenever weighted parameter β turned out to be zero, the closed trajectory becomes tangent at $(AT, c/q)$ with extreme vertical coordinate. In this case, if the fixed point exists then it must belong to the basic phase set $(\tau, (c/q) + \tau]$. We will demonstrate that under what condition the fixed point of the Poincaré map belongs to the maximum phase set $(\tau, (c/q) + \tau]$. We have the following two positions for A_l, i.e., (i) $A_l \le 0$ and (ii) $A_l > 0$. If $A_l \le 0$, then it can easily be shown that $y^* > \tau$ and furthermore, the inequality

$$y^* = \tau \frac{\exp((q/c)\tau - (A_l/c))}{\exp((q/c)\tau - (A_l/c)) - 1} \le \frac{c}{q} + \tau \tag{71}$$

holds true. This shows that if $A_l \le 0$, then $y^* \in (\tau, (c/q) + \tau]$. If $A_l > 0$, then the fixed point exists provided that $\exp((q/c)\tau - (A_l/c)) > 1$. This also ensures that y^* is positive and greater than τ. We take

$$y^* = \tau \frac{\exp((q/c)\tau - (A_l/c))}{\exp((q/c)\tau - (A_l/c)) - 1} \le \frac{c}{q} + \tau, \tag{72}$$

which is equivalent to

$$\exp\left(\frac{q}{c}\tau - \frac{A_l}{c}\right) \ge \frac{q}{c}\tau + 1. \tag{73}$$

The following inequality can easily be obtained after simple rearrangement

$$-\frac{q}{c}\left(\frac{c}{q} + \tau\right)\exp\left[-\frac{q}{c}\left(\frac{c}{q} + \tau\right)\right] \ge -\exp\left(-1 - \frac{A_l}{c}\right). \tag{74}$$

Solving inequality (74) with respect to $(c/q) + \tau$ gives either $(c/q) + \tau \le y_{\min}^2$ or $(c/q) + \tau \ge y_{\max}^2$. The first inequality is impossible due to $y_{\min}^2 \le (c/q)$. This shows that $(c/q) + \tau \ge y_{\max}^2$, and hence $y^* \le (c/q) + \tau$ when $0 < A_l < q\tau$.

If weighted parameter $\beta > 0$, the tangency point of the closed trajectory moves to some other point having vertical coordinate less than c/q, and in this case, the basic impulsive set can be written as $(\tau, (c/q) + \tau)$ or $(\tau, y_T + \tau]$, where $y_T < c/q$. This shows that $y^* < (c/q) + \tau$ or $y^* \le y_T + \tau$ when $0 < A_l < q\tau$.

In the following discussion, we give some important relations related to y_{im}^1, y_{im}^3, $y_{\max}^2$, $y_{\min}^3$ and $y_{\max}^3$.

Lemma 7. *If $0 < A_l < q\tau$ and $\beta = 0$, then y^* attains its minimal value $y_{\min}^* = y_{\max}^2$ at $\tau_1 = y_{\max}^2 - c/q$. If $\beta > 0$, then y^* attains its minimal value $y_{\min}^* = y_{\max}^2$ at $\tau_1 = y_{\max}^2 - y_T$ where $y_T < c/q$.*

Proof. Taking the derivative of y^* with respect to τ, we get

$$\frac{dy^*}{d\tau} = \frac{\exp((q/c)\tau - (A_l/c))[c\exp((q/c)\tau - (A_l/c)) - c - q\tau]}{c[\exp((q/c)\tau - (A_l/c)) - 1]^2}. \tag{75}$$

Let $(dy^*/d\tau) = 0$, then the above equality becomes

$$c\exp\left(\frac{q}{c}\tau - \frac{A_l}{c}\right) - c - q\tau = 0. \tag{76}$$

From (76), we get

$$\left(-1 - \frac{q\tau}{c}\right)\exp\left(-1 - \frac{q\tau}{c}\right) = -\exp\left(-1 - \frac{A_l}{c}\right). \tag{77}$$

We can solve the above equation with the help of Lambert W function. It will give us two solutions; however, only the larger solution is positive. The necessary condition for the positivity is $A_l < q\tau$. If we denote the positive root by τ_1, we get

$$\tau_1 = -\frac{c}{q} - \frac{c}{q}W\left(-1, -e^{-1-A_l/c}\right) = y_{\max}^2 - \frac{c}{q}. \tag{78}$$

It is obvious that y^* attains its minimal value at τ_1, and as $\tau \to A_l/q$, $y^* \to \infty$. By simple calculations, it can be shown that $\exp((q/c)\tau_1 - (A_l/c)) = -W\left(-1, -e^{-1-A_l/c}\right)$. Finally, by putting this in (70) we get

$$y_{\min}^* = \tau_1 \frac{W\left(-1, -e^{-1-A_l/c}\right)}{1 + W\left(-1, -e^{-1-A_l/c}\right)} = -\frac{c}{q}W\left(-1, -e^{-1-A_l/c}\right) = y_{\max}^2. \tag{79}$$

For $\beta = 0$, if we take $(c/q) + \tau - y^* = 0$ then substituting the value of y^* and using the equality (76) it can easily be shown that $c/q + \tau$ and y^* intersect each other at $\tau = \tau_1$. For Case (C_2), if $\beta > 0$ then it can be seen that y^* attains its minimum value at $\tau = \tau_1$, where $\tau_1 = y_{\max}^2 - y_T$.

Lemma 8. *If $A_l \le 0$, then for the fixed point y^* the following inequality is satisfied*

$$y^* < \frac{c + q\tau + \sqrt{c^2 + q^2\tau^2}}{2q}. \tag{80}$$

Proof.

$$y^* = \tau\frac{\exp((q/c)\tau - (A_l/c))}{\exp((q/c)\tau - (A_l/c)) - 1} \le \tau\frac{\exp((q/c)\tau)}{\exp((q/c)\tau) - 1} < \frac{c + q\tau + \sqrt{c^2 + q^2\tau^2}}{2q}. \tag{81}$$

After simple rearrangement, we get

$$\left(c + \sqrt{c^2 + q^2\tau^2} - q\tau\right)\exp\left[\frac{q}{c}\tau\right] - c - q\tau - \sqrt{c^2 + q^2\tau^2} > 0. \tag{82}$$

Let $h = (q/c)\tau$, then the above inequality can be rewritten as

$$e^h > \frac{1 + h + \sqrt{1 + h^2}}{1 - h + \sqrt{1 + h^2}} = h + \sqrt{1 + h^2}. \tag{83}$$

To complete the proof, it is enough to show that $e^h - h - \sqrt{1 + h^2} > 0$.

Consider the function $F(h) = e^h - h - \sqrt{1 + h^2}$, and we have

$$F(h) = e^h - h - \sqrt{1 + h^2} > 1 + h + \frac{h^2}{2} - \left(h + \sqrt{1 + h^2}\right) = 1 + \frac{h^2}{2} - \sqrt{1 + h^2} > 0. \tag{84}$$

Hence, if $A_l \le 0$ then the inequality (80) is true. □

Lemma 9. *Positive solutions of the following equations exist*

$$(i)\quad y^* - y_{\max}^3 = 0; \quad (ii)\quad y^* - y_{\min}^3 = 0. \tag{85}$$

Proof. (i)Let $y^* - y_{\max}^3 = 0$, then substituting the value of y^* and after simple rearrangement we get

$$\frac{q}{c}\left(\tau - y_{\max}^3\right)\exp\left(\frac{q}{c}\left(\tau - y_{\max}^3\right)\right) = -\frac{q}{c}y_{\max}^3\exp\left(-\frac{q}{c}y_{\max}^3 + \frac{A_l}{c}\right). \tag{86}$$

By putting the value of $y_{\max}^3$, we get

$$-\frac{q}{c}y_{\max}^3\exp\left(-\frac{q}{c}y_{\max}^3 + \frac{A_l}{c}\right) = -e^{-1}e^{-(A_u - A_l)/c} = -e^{-1-A_v/c} \tag{87}$$

i.e.,

$$\frac{q}{c}\left(\tau - y_{\max}^3\right)\exp\left(\frac{q}{c}\left(\tau - y_{\max}^3\right)\right) = -e^{-1-A_v/c}. \tag{88}$$

The above equation can be solved with the help of Lambert W function and yields two solutions

$$\tau_2 = y_{\max}^3 + \frac{c}{q}W\left(-1, -e^{-1-A_v/c}\right) \text{ and } \tau_3 = y_{\max}^3 + \frac{c}{q}W\left(-e^{-1-A_v/c}\right). \tag{89}$$

Since $A_v \ge 0$, which implies $A_u \ge A_l > 0$ or $A_u > 0 \ge A_l$. This shows that the above solutions are well defined. If $A_l \le 0$, then the small root τ_2 disappeared and subsequently in this case, we only get the root τ_3 which can also be written as $\tau_3 = y_{\max}^3 - y_{im}^3$.

Following the same way, it can easily be shown that if $A_l \le 0$ then the unique positive solution exists for the equation (ii) is $\tau_4 = y_{\min}^3 + (c/q)W\left(-e^{-1-A_v/c}\right)$. This solution can also be expressed as $\tau_4 = y_{\min}^3 - y_{im}^3$.

5.2. Existence and Stability of Boundary Order-1 Periodic Solution. This subsection focuses on the existence and stability of fixed point of Poincaré map $P(y_i^+)$ for special case $\tau = 0$. The analytical formula for Poincaré map $P(y_i^+)$ is already formed in Section 4. Let y^* be the fixed point of Poincaré map $P(y_i^+)$, then we have $y^* = P(y^*)$, i.e.,

$$y^* = -\frac{c}{q}W\left[-\frac{q}{c}y^*\left(\exp\left(-\frac{q}{c}y^* + \frac{A_l}{c}\right)\right)\right]. \tag{90}$$

To determine the fixed point, we take the following two cases for A_l, (1) $A_l = 0$ and (2) $A_l \ne 0$. For the first case, equation (90) reduced into

$$y^* = -\frac{c}{q}W\left[-\frac{q}{c}y^*\left(\exp\left(-\frac{q}{c}y^*\right)\right)\right], \tag{91}$$

by using the properties of Lambert W function, the equation (91) can be expressed as $-(q/c)y^*e^{-(q/c)y^*} = -(q/c)y^*e^{-(q/c)y^*}$. This shows that y^* is the fixed point of Poincaré map $P(y_i^+)$.

For the second case, we get $-(q/c)y^*e^{-(q/c)y^*} = -(q/c)y^*e^{-(q/c)y^* + A_l/c}$. This equality is satisfied if and only if $y^* = 0$. Hence, the only fixed point exists for the Poincaré map is $y^* = 0$.

In the above discussion, we have demonstrated that the fixed point of Poincaré map exists. We will now inspect that under what condition the boundary order-1 periodic solution is globally stable. To prove it, we first recall a lemma from [48, 49].

Lemma 10. *The T-periodic solution $(x, y) = (\zeta(t), \xi(t))$ of system*

$$\begin{cases} \frac{dx}{dt} = L(x,y), \quad \frac{dy}{dt} = M(x,y), \quad \text{if } \varphi(x,y) \neq 0, \\ x^+ = x + \alpha_1(x,y), \quad y^+ = y + \beta_1(x,y), \quad \text{if } \varphi(x,y) = 0 \end{cases} \tag{92}$$

is orbitally asymptotically stable if the Floquet multiplier μ_2 satisfies the condition $|\mu_2| < 1$, where

$$\mu_2 = \prod_{j=1}^{k} \Delta_j \exp\left(\int_0^T \left[\frac{\partial L}{\partial x}(\zeta(t),\xi(t)) + \frac{\partial M}{\partial y}(\zeta(t),\xi(t)) \right] dt \right) \tag{93}$$

with

$$\Delta_j = \frac{L_+\left((\partial\beta_1/\partial y)(\partial\varphi/\partial x) - (\partial\beta_1/\partial x)(\partial\varphi/\partial y) + (\partial\varphi/\partial x)\right) + M_+\left((\partial\alpha_1/\partial x)(\partial\varphi/\partial y) - (\partial\alpha_1/\partial y)(\partial\varphi/\partial x) + (\partial\varphi/\partial y)\right)}{L(\partial\varphi/\partial x) + M(\partial\varphi/\partial y)}, \tag{94}$$

and φ is continuously differentiable with respect to x, y. $L, M, \partial\alpha_1/\partial x, \partial\alpha_1/\partial y, \partial\beta_1/\partial x, \partial\beta_1/\partial y, \partial\varphi/\partial x$, and $\partial\varphi/\partial y$ are calculated at point $\left(\zeta(t_j), \xi(t_j)\right)$, $L_+ = L\left(\zeta(t_j^+), \xi(t_j^+)\right)$ and $M_+ = M\left(\zeta(t_j^+), \xi(t_j^+)\right)$, and t_j ($j, k \in N$, N is the set of nonnegative integers) is the time of the j-th jump.

Theorem 2. *Let $\tau = 0$ and $A_l = (\lambda/\omega)\ln((1 + \omega(AT/(\alpha + c\beta)))/(1 + \omega(AT/(\alpha + c\beta))(1 - p))) - r(AT/(\alpha + c\beta)) p + \delta\ln(1 - p) \neq 0$. Then boundary order-1 periodic solution $\left(x^T(t), 0\right)$ of system (2) is globally asymptotically stable for Case (C_1), and locally asymptotically stable for Case $(C_3)(ii)$. For Cases (C_2) and $(C_3)(i)$, the boundary order-1 periodic solution is unstable.*

Proof. In the following lines, we first prove that the boundary order-1 periodic solution $\left(x^T(t), 0\right)$ exists for system (2) when $y(t) = 0$ if and only if $\tau = 0$. For $y(t) = 0$, the system (2) transformed into the following subsystem:

$$\begin{cases} \frac{dx(t)}{dt} = cx(t), \quad x(t) < \frac{AT}{\alpha + c\beta}, \\ x(t^+) = (1 - p)x(t), \quad x(t) = \frac{AT}{\alpha + c\beta}. \end{cases} \tag{95}$$

Combining the first equation of subsystem (95) with initial condition $x(0^+) = (1 - p)(AT/\alpha + c\beta)$ gives us the solution

$$x(t) = (1 - p)\frac{AT}{\alpha + c\beta}\exp(ct). \tag{96}$$

Taking $(AT/\alpha + c\beta) = (1 - p)(AT/\alpha + c\beta)\exp(cT)$ and evaluating it for T, we get $T = -(1/c)\ln(1 - p)$. This confirms that T-periodic boundary order-1 solution exists for system (2) as follows:

$$\left(x^T(t), 0\right) = \left((1 - p)\frac{AT}{\alpha + c\beta}\exp(ct), 0\right). \tag{97}$$

Next, we present the global attractivity of the boundary order-1 periodic solution $\left(x^T(t), 0\right)$ for Case (C_1). Let $p_0^+ = ((AT(1 - p))/(\alpha + c\beta), y_i^+) \in L_3$ and $p_1 = (AT/(\alpha + c\beta), y_{i+1}) \in L_2$ be points of the same trajectory, then for these points the following relation is satisfied

$$\begin{aligned} A_l &= \frac{\lambda}{\omega}\ln\frac{1 + \omega(AT/(\alpha + c\beta))}{1 + \omega(AT/(\alpha + c\beta))(1 - p)} - r\frac{AT}{\alpha + c\beta}p + \delta\ln(1 - p) \\ &= c\ln\frac{y_{i+1}}{y_i^+} - q(y_{i+1} - y_i^+). \end{aligned} \tag{98}$$

Since $A_l \neq 0$, so $y_{i+1} \neq y_i^+$. Let us define a function $f(y) = c\ln y - qy$, then $f'(y) = (c/y) - q$. This shows that $f(y)$ is monotonically increasing for all those values y of the domain such that $y < c/y$.

If $A_l < 0$, then $c\ln(y_{i+1}/y_i^+) - q(y_{i+1} - y_i^+) < 0$. Since $\tau = 0$, so the inequality can be rewritten as $c\ln(y_{i+1}/y_i) - q(y_{i+1} - y_i) < 0$. From this, it is clear that $y_{i+1} < y_i$. Hence, if $A_l \leq 0$ then the impulsive sequence $\{y_k^+\}_{k=0}^{\infty}$ is monotonically decreasing and satisfies $\lim_{k\to\infty} y_k^+ = y^*$. This confirms that boundary order-1 periodic solution for Case (C_1) is globally attractive. Following the same way, it can easily be shown that if $A_l > 0$ then $y_{i+1} > y_i$. Consequently, for Cases (C_2) and $(C_3)(i)$ the sequence y_k^+ will be free from impulsive effect after the finite time pulse actions, as shown in Figure 4(a).

Now, we demonstrate that boundary order-1 periodic solution is asymptotically stable. To do this, we employ Lemma 10 and denote

Method 1:

$$\begin{aligned} L(x,y) &= (c - qy)x, \quad M(x,y) = \left(\tfrac{\lambda x}{1+\omega x} - rx - \delta\right)y, \\ \alpha_1(x,y) &= -px, \quad \beta_1(x,y) = \tau, \quad \varphi(x,y) = (\alpha + c\beta)x - q\beta xy - AT, \\ \left(x^T(T), y^T(T)\right) &= \left(\tfrac{AT}{\alpha+c\beta}, 0\right), \quad \left(x^T(T^+), y^T(T^+)\right) = \left((1 - p)\tfrac{AT}{\alpha+c\beta}, 0\right). \end{aligned} \tag{99}$$

From above, we can easily calculate:

$$\begin{aligned} \frac{\partial L}{\partial x} &= c - qy, \quad \frac{\partial M}{\partial y} = \frac{\lambda x}{1+\omega x} - rx - \delta, \frac{\partial\alpha_1}{\partial x} = -p, \\ \frac{\partial\varphi}{\partial x} &= \alpha + c\beta - q\beta y, \quad \frac{\partial\varphi}{\partial y} = -q\beta x, \quad \frac{\partial\alpha_1}{\partial y} = \frac{\partial\beta_1}{\partial x} = \frac{\partial\beta_1}{\partial y} = 0, \end{aligned} \tag{100}$$

and

$$\begin{aligned} \Delta_1 &= \frac{L_+\left((\partial\beta_1/\partial y)(\partial\varphi/\partial x) - (\partial\beta_1/\partial x)(\partial\varphi/\partial y) + (\partial\varphi/\partial x)\right) + M_+\left((\partial\alpha_1/\partial x)(\partial\varphi/\partial y) - (\partial\alpha_1/\partial y)(\partial\varphi/\partial x) + (\partial\varphi/\partial y)\right)}{L(\partial\varphi/\partial x) + M(\partial\varphi/\partial y)} \\ &= \frac{L^+\left(x^T(T^+), y^T(T^+)\right)(\alpha + c\beta - q\beta y) + M^+\left(x^T(T^+), y^T(T^+)\right)(pq\beta x - q\beta x)}{L\left(x^T(T), y^T(T)\right)(\alpha + c\beta - q\beta y) - M\left(x^T(T), y^T(T)\right)(q\beta x)} \\ &= (1 - p). \end{aligned} \tag{101}$$

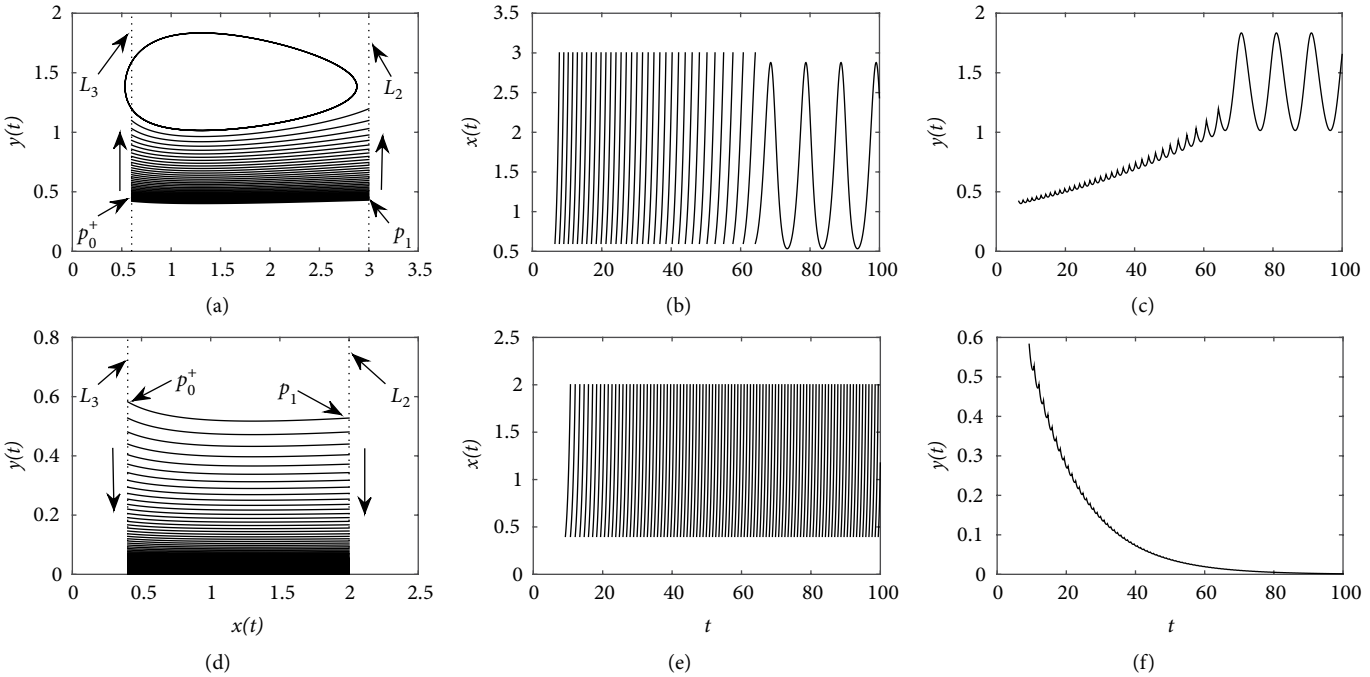

FIGURE 4: (a–c) Unstable boundary order-1 periodic solution with $L_2 = AT/(\alpha + c\beta) = 3$, $AT = 3.24$ and $A_l = 0.02643$; (d–f) stable boundary order-1 periodic solution with $L_2 = 2$, $AT = 2.16$ and $A_l = -0.106676$. All other parameter values are fixed as: $c = 1.8, q = 1.3, \lambda = 0.52, \omega = 0.1, r = 0.23, \delta = 0.3, \alpha = 0.9, \beta = 0.1, p = 0.8, \tau = 0$.

In addition, we also have

$$\begin{aligned}
&\exp\left(\int_0^T\left[\frac{\partial L}{\partial x}\left(x^T(t), y^T(t)\right) + \frac{\partial M}{\partial y}\left(x^T(t), y^T(t)\right)\right]dt\right)\\
&= \exp\left(\int_0^T\left[c + \frac{\lambda(1-p)(AT/(\alpha+c\beta))\exp(ct)}{1+\omega(1-p)(AT/(\alpha+c\beta))\exp(ct)} - r(1-p)\frac{AT}{\alpha+c\beta}\exp(ct) - \delta\right]dt\right)\\
&= \exp\left(\ln\frac{1}{(1-p)} + \frac{\lambda}{c\omega}\ln\left(\frac{1+\omega(AT/(\alpha+c\beta))}{1+\omega(AT/(\alpha+c\beta))(1-p)}\right) - \frac{r}{c}\frac{AT}{\alpha+c\beta}p + \frac{\delta}{c}\ln(1-p)\right)\\
&= \exp\left(\ln\frac{1}{(1-p)} + \frac{A_l}{c}\right).
\end{aligned} \tag{102}$$

The Floquet multiplier μ_2 can be found as:

$$\begin{aligned}
\mu_2 &= \Delta_1\exp\left(\int_0^T\left[\frac{\partial L}{\partial x}\left(x^T(t), y^T(t)\right) + \frac{\partial M}{\partial y}\left(x^T(t), y^T(t)\right)\right]dt\right)\\
&= (1-p)\exp\left(\ln\frac{1}{1-p} + \frac{A_l}{c}\right)\\
&= \exp\left(\frac{A_l}{c}\right).
\end{aligned} \tag{103}$$

If $A_l < 0$ and $\tau = 0$, then from last equation we can see that $|\mu_2| < 1$. This shows that the boundary order-1 periodic solution $\left(x^T(t), 0\right)$ of system (2) is orbitally asymptotically stable for Case (C_1). From the domain of phase set, it is also obvious that the boundary order-1 periodic solution is locally asymptotically stability for Case $(C_3)(ii)$. For Cases (C_2) and $(C_3)(i)$, the sequence y_k^+ of impulsive points is strictly increasing, and it will be free from impulsive effect after a finite number of pulse actions.

In order to inspect the results shown in Theorem 2 and the effects of A_l, we fixed all the parametric values as those appeared in Figure 4. The numerical calculation in Figures 4(a)–4(c) verifies that if $A_l \geq 0$, then the boundary order-1 periodic solution is unstable while Figures 4(d)–4(f) confirms that if $A_l < 0$, then it is stable.

Method 2: The local stability of the boundary order-1 periodic solution can also be obtained from the definition of Poincaré map obtained in (56). Let $\tau = 0$, then we have

$$P(y_i^+) = -\frac{c}{q}W\left[-\frac{q}{c}y_i^+\left(\exp\left(-\frac{q}{c}y_i^+ + \frac{A_l}{c}\right)\right)\right]. \tag{104}$$

Taking the derivative of equation (104), we get

$$\begin{aligned}
\left.\frac{dP(y_i^+)}{dy_i^+}\right|_{y_i^+=y^*} &= \left.\frac{d}{dy_i^+}\right|_{y_i^+=y^*}\left(-\frac{c}{q}W\left[-\frac{q}{c}y_i^+\left(\exp\left(-\frac{q}{c}y_i^+ + \frac{A_l}{c}\right)\right)\right]\right)\\
&= \frac{(-c/q)W[(-q/c)y^*(\exp((-q/c)y^* + A_l/c))]}{1 + W[(-q/c)y^*(\exp((-q/c)y^* + A_l/c))]}\left(\frac{1}{y^*} - \frac{q}{c}\right) = h(y^*).
\end{aligned} \tag{105}$$

The boundary order-1 periodic solution is stable if and only if the absolute value of $h(y^*)$ is less than one. By taking limit of $h(y^*)$, we get

$$\lim_{y^*\to 0} h(y^*) = e^{A_l/c}. \tag{106}$$

This limit shows that if $A_l < 0$, then $|h(y^*)| < 1$ as $y^* \to 0$, thus the boundary order-1 periodic solution is asymptotically stable. Hence, from all the above outcomes, it can be concluded that boundary order-1 periodic solution $\left(x^T(t), 0\right)$ is globally asymptotically stable. This completes the proof. □

6. Characterization of Periodic Solution for $\tau > 0$

In this section, we aim to give the detailed conditions for the existence and stability of the fixed point of Poincaré map $P(y_i^+)$. From above discussion, it is obvious that the impulsive and phase sets are complex curves that rely upon the weighted parameters α and β. So, we will perceive how these parameters

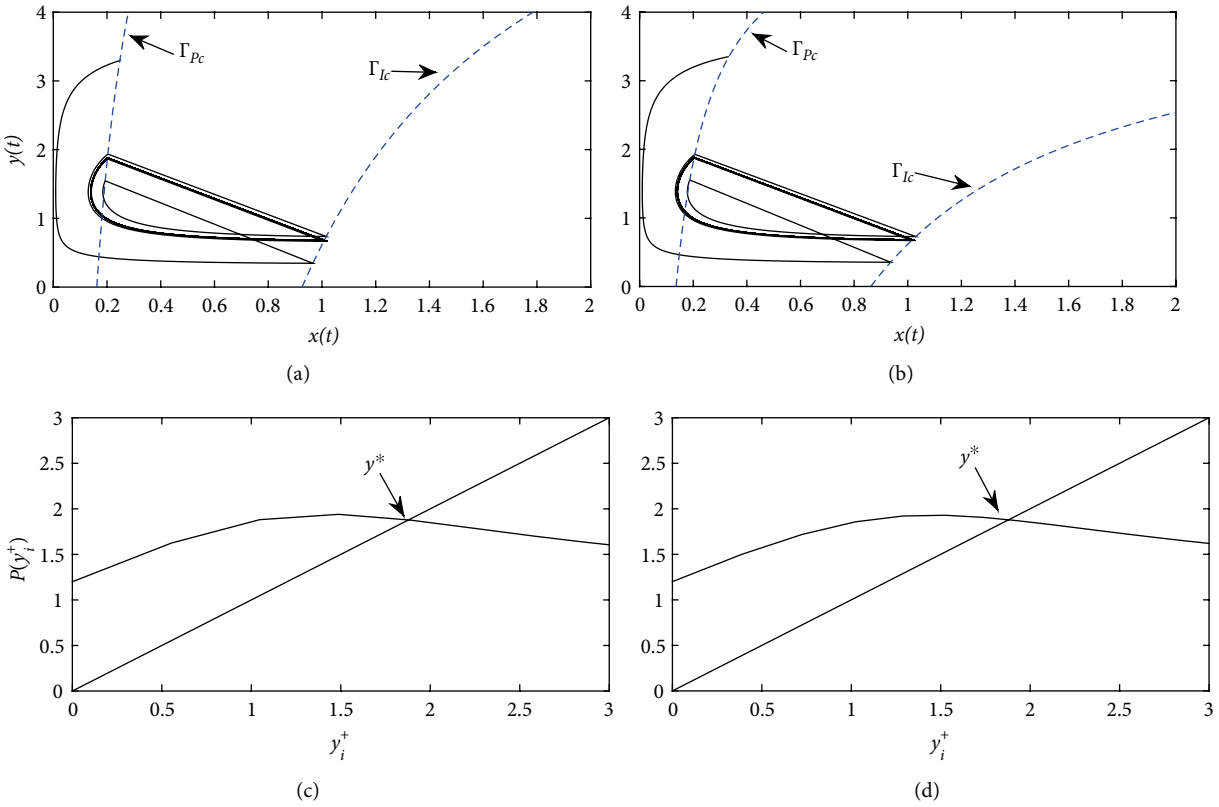

FIGURE 5: Fixed point of Poincaré map for Case (C_1). All other parametric values are fixed as: $c = 1.8, q = 1.3, \lambda = 0.52, \omega = 0.1, r = 0.23, \delta = 0.3, p = 0.8, \tau = 1.2, AT = 1$. (a) $\beta = 0.1$, $y^* = 1.8784$, (b) $\beta = 0.1$, (c) $\beta = 0.2$, $y^* = 1.8789$, (d) $\beta = 0.2$.

differ our results from literature [42]. We first find out the conditions that ensure the existence of order-1 periodic solution for system (2).

6.1. Existence of Order-1 Periodic Solution. In order to achieve the target, we first give an important lemma which will be used in the upcoming results.

Lemma 11. *If $A_l > 0$ and $\tau > 0$, then the following inequality is satisfied for the Poincaré map $P(y_i^+)$*

$$P(y_i^+) > y_i^+, \quad \text{for all} \quad y_i^+ \in (0, y_{P_2}). \tag{107}$$

Proof. Let a trajectory originate from $p_0^+ = (x_i^+, y_i^+)$ and it touches curve Γ_{Ic} at point $p_1 = (x_{i+1}, y_{i+1})$. Here, we assume that $y_i^+, y_{i+1} < c/q$, then these points must satisfy the relation:

$$\frac{\lambda}{\omega}\ln\frac{1+\omega x_{i+1}}{1+\omega x_i^+} - r(x_{i+1} - x_i^+) - \delta\ln\frac{x_{i+1}}{x_i^+} = c\ln\frac{y_{i+1}}{y_i^+} - q(y_{i+1} - y_i^+). \tag{108}$$

From (107), we get

$$-\frac{q}{c}y_{i+1}e^{(-(q/c)y_{i+1})} = -\frac{q}{c}y_i^+e^{(-(q/c)y_i^* + A_l/c)}. \tag{109}$$

If $A_l > 0$, then we get the inequality

$$-\frac{q}{c}y_{i+1}e^{(-(q/c)y_{i+1})} < -\frac{q}{c}y_i^+e^{(-(q/c)y_i^+)}. \tag{110}$$

Let us define $f(y) = -y\exp(-y)$, then $f'(y) > 0$ if $y > 1$ and $f'(y) < 0$ if $y \in (0, 1)$. The inequality $y_{i+1} \geq y_i^+$ is satisfied for all $(q/c)y_i^+, (q/c)y_{i+1} \in (0, 1)$. We also know that $y_{i+1}^+ = y_{i+1} + \tau$ and $P(y_i^+) = y_{i+1}^+$. From the above discussions, we conclude that $P(y_i^+) > y_i^+$ for all $y_i^+ \in (0, y_{P_2})$. □

Theorem 3. *For Case (C_1), the fixed point of Poincaré map $P(y_i^+)$ exists and therefore periodic solution of order-1 exists for system (2), as shown in Figure 5.*

Proof. Let a trajectory Γ_1 is tangent at point (x_S, y_S) and it touches curve Γ_{Ic} at point (x_{Q_2}, y_{Q_2}), such that $y_{Q_2} < c/q$.

If $P(y_S) = y_{Q_2}^+$, then clearly curve $\overset{\frown}{SQ_2}$ forms an order-1 periodic solution. If $P(y_S) \neq y_S$, then either $P(y_S) > y_S$ or $P(y_S) < y_S$.

If $P(y_S) > y_S$, then trajectory originating from point $P(y_S) = y_{Q_2}^+$ will touch curve Γ_{Ic} at point y_{Q_3}. After one time pulse action, it will be adjusted at point $P(y_{Q_2}^+) = y_{Q_3}^+$. Hence, we get the inequality

$$P(y_{Q_2}^+) < y_{Q_2}^+. \tag{111}$$

For the second case, the following inequality is satisfied

$$P(y_S) < y_S. \tag{112}$$

We also know that for the lowest impulsive point τ, the following inequality is always satisfied

$$P(\tau) > \tau. \tag{113}$$

From (111) and (113), due to continuity of the Poincaré map we see that the fixed point exists in the interval $\left(\tau, y^{+}_{Q_2}\right)$ and from (112) and (113), we can see that the fixed point for Poincaré map exists in the interval (τ, y_S). □

Theorem 4. *For Case (C_2), if $P\left(y_{P_1}\right) > y_{P_1}$ then the fixed point of the Poincaré map $P\left(y_i^{+}\right)$ exists above the point y_{P_1} and therefore periodic solution of order-1 exists for system (2).*

Proof. For Case (C_2), there exists a trajectory which touches curve Γ_{Pc} at two points $\left(x_{P_1}, y_{P_1}\right)$ and $\left(x_{P_2}, y_{P_2}\right)$ and tangents to curve Γ_{Ic} at point $T = (x_T, y_T)$. If $P\left(y_{P_1}\right) = y_{T^+} = y_{P_1}$, then curve $\widehat{P_1T}$ forms an order-1 periodic solution for system (2). If $P\left(y_{P_1}\right) \neq y_{P_1}$, then either $P\left(y_{P_1}\right) > y_{P_1}$ or $P\left(y_{P_1}\right) < y_{P_1}$.

If $P\left(y_{P_1}\right) > y_{P_1}$, then trajectory originating from point $P\left(y_{P_1}\right) = y_{T^+}$ touches curve Γ_{Ic} having vertical coordinate y_{T_1} which is less than y_T, i.e., $y_{T_1} < y_T$. Then after one time pulse action, we get $y^{+}_{T_1}$. It can easily be seen that $y^{+}_{T_1} < y^{+}_{T}$. Hence, we get the inequality

$$P\left(y_{T^+}\right) < y_{T^+}. \tag{114}$$

For this case, we already know that

$$P\left(y_{P_1}\right) > y_{P_1}. \tag{115}$$

Combining the inequalities (114) and (115), it is obvious that the fixed point of the Poincaré map exists in the interval $\left(y_{P_1}, y_{T^+}\right)$ and hence periodic solution of order-1 exists for system (2). This completes the proof. □

If $P\left(y_{P_1}\right) < y_{P_1}$, then any trajectory initiating from Γ_{Pc} will touch curve Γ_{Ic} and after one time pulse action, it will move to the interval $[\tau, y_{T^+}]$. If $\tau > y_{P_2}$, then trajectory starting from y^{+} will directly move inside the closed trajectory after one time pulse action and it will be free from additional impulsive effect. If $\tau \leq y_{P_2}$, then using the inequality (107) any trajectory originating from y^{+} with $y^{+} \in \left[\tau, y_{P_2}\right]$ will reach at curve Γ_{Ic} and after a limited number of pulse actions it will finally enter into the closed trajectory Γ_2, and there will be no more pulse actions on it. Thus, for this case, no fixed point of the Poincaré map exists and, therefore, no periodic solution of order-1 exists for system (2). □

Theorem 5. *For Case $(C_3)(i)$, if $\tau > \tau_3$ then the fixed point of the Poincaré map $P\left(y_i^{+}\right)$ exists above the point y_{P_1}. For Case $(C_3)(ii)$, if $\tau < \tau_4\ (\tau > \tau_3)$ then the fixed point exists below the point y_{P_2} (above y_{P_1}) and therefore periodic solution of order-1 exists for system (2), as shown in Figure 3.*

Proof. For Case $(C_3)(i)$, the homoclinic trajectory Γ_3 touches with curve Γ_{Pc} at two points $\left(x_{P_1}, y_{P_1}\right)$ and $\left(x_{P_2}, y_{P_2}\right)$ and its right lower branch touches curve Γ_{Ic} at point $\left(x_{Q_2}, y_{Q_2}\right)$. It is obvious that $y_{Q_2} < c/q$. If $\tau = \tau_3$, then we can see that y^{*}, $y^{+}_{Q_2}$ and y_{P_1} meet each other. If $\tau > \tau_3$, then from the relation (i) of Lemma 9, we conclude that the fixed point lies above point y_{P_1}.

Table 1: Exact domains of the fixed point of Poincaré map $P(y_i^{+})$ for system (2).

Cases	Condition	τ	Interval of y^{*}
(C_1)	$A_l \leq 0$	$\tau > 0$	$\left[\tau, y^{1}_{im} + \tau\right]$
(C_2)	$A_l > 0$	$\tau \geq \tau_1$	$\left[y^{2}_{\max}, y_T + \tau\right]$
(C_3)	(i)$A_u \geq A_l < 0$	$\tau > \tau_3$	$\left(y^{3}_{\max}, y^{3}_{im} + \tau\right]$
	(ii)$A_u \geq 0, A_l \leq 0$	$0 < \tau < \tau_4$	$\left(0, y^{3}_{\min}\right)$
	(iii)$A_u \geq 0, A_l \leq 0$	$\tau > \tau_3$	$\left(y^{3}_{\max}, y^{3}_{im} + \tau\right]$

If $\tau < \tau_4$, then following the relation (ii) of Lemma 9, we conclude that the fixed point must be less than y_{P_2} and hence belongs to the interval $\left(0, y_{P_2}\right)$. If $\tau > \tau_3$, then following the same way as in Case $(C_3)(i)$, it can be shown that the fixed point lies above point y_{P_1}. Hence, an order-1 periodic solution exists for system (2). □

Corollary 2. *For Case $(C_3)(ii)$, if $\tau_4 < \tau < \tau_3$ then any trajectory originating from the $\left(x_0^{+}, y_0^{+}\right)$, will move inside the trajectory Γ_3 after one time pulse action and there will be no more pulse action on it.*

Corollary 3. *For Case $\left(C_1^0\right)$, if $\tau > 0$ then for model (8) the fixed point of the Poincaré map exists in the interval $\left[\tau, y^{1}_{im} + \tau\right]$. For Case $\left(C_2^0\right)$, if $P\left(y_{P_1}\right) > y_{P_1}$ then the fixed point exists in the interval $\left[y^{0}_{\max}, y_{T_0} + \tau\right]$.*

Based on all the information given above, we give the exact domains of the fixed points of the Poincaré map in terms of y_T, $y^{2}_{\max}$, $y^{3}_{\min}$, $y^{3}_{\max}$, y^{1}_{im}, y^{3}_{im} in Table 1.

6.2. Effect of Weighted Parameters on the Dynamic Behavior of System (2). It is already discussed in detail that under what conditions the fixed point of Poincaré map exists for all existing cases. In the present paper, we have proposed a system with ratio-dependent AT, i.e., instead of vertical straight lines we have complex curves depends on the weighted parameters α and β. These complex curves change their position with a little increase or decrease in the weighted parameters.

Figures 5–8 reveal the detailed description of the behavior of fixed point y^{*}. The fixed point of Poincaré map is affected by the weighted parameters α and β. From Figure 5, we can see that the fixed point of Poincaré map is increasing monotonically for Case (C_1). For this case, the minimum fixed point we get whenever weighted parameter $\beta = 0$, i.e., the threshold is only pest density dependent and as β increases the fixed point also increases monotonically. The numerical simulation shows that the fixed point of Poincaré map either increases or decreases monotonically.

The diagrams appearing in Figures 6 and 8 describe that the Poincaré map is quite complex in these cases. The fixed points of Poincaré map change as the weighted parameters vary. The diagrams shown in Figure 6 is more complex and amazing. For Case (C_2), once the weighted parameter β increases, the fixed point of Poincaré map also increases monotonically, and the fixed point of Poincaré map starts decreasing dramatically as β reaches 0.6. Specifically, it is

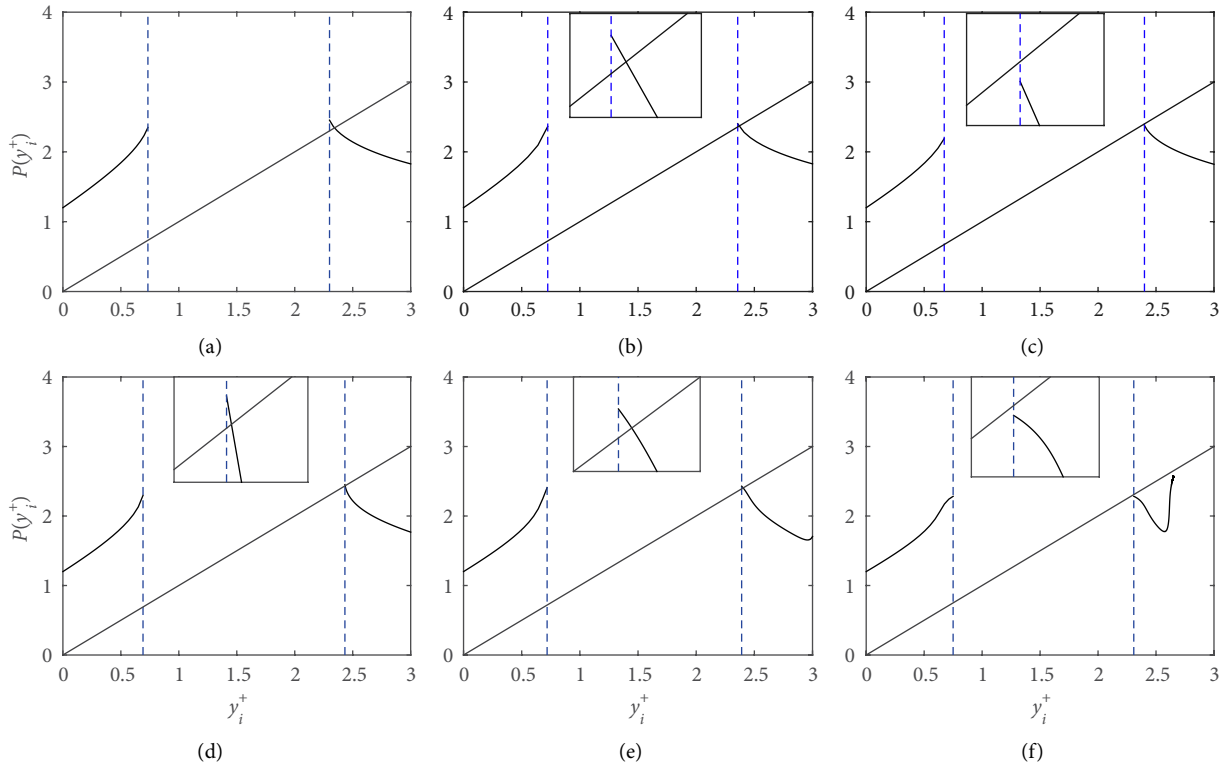

FIGURE 6: Effect of weighted parameters on the fixed point of Poincaré map for Case (C_2). (a) $\beta = 0$, (b) $\beta = 0.1$, (c) $\beta = 0.2$, (d) $\beta = 0.4$, (e) $\beta = 0.6$, and (f) $\beta = 0.9$. All other parametric values are fixed as: $c = 1.8$, $q = 1.3$, $\lambda = 0.52$, $\omega = 0.1$, $r = 0.23$, $\delta = 0.3$, $p = 0.8$, $\tau = 1.2$, $AT = 6$.

interesting to note that once β becomes greater than 0.1, the fixed point disappears and it reappears when β crosses the value 0.3. At 0.4, it converts into Case (C_3) and when β approaches 1 and α is small enough, the fixed point of Poincaré map again disappears, for example, Figure 6(f).

From Figure 7, we can also see that how the value of A_l varies only by a small change in the weighted parameters. For this case, if the weighted parameter β increases the fixed point of Poincaré map decreases monotonically, and there does not exist any fixed point once β becomes greater than 0.2, for example, Figures 8(c) and 8(d).

6.3. Local and Global Stability of Order-1 Periodic Solution. In this subsection, in the light of the above results, we will examine the local and global stability of the fixed point of Poincaré map $P(y_i^+)$. To show these results, we suppose that $\tau > 0$ and y^* exists.

Theorem 6. *If $A_l \le 0$, then for model (2) the fixed point of Poincaré map is locally stable. If $A_l > 0$, then the fixed point of Poincaré map is locally stable provided that $y^* < \left(c + q\tau + \sqrt{c^2 + q^2\tau^2}\right)/2q$.*

Proof. Let y^* be the fixed point of Poincaré map, and let $g(y) = -(q/c)y\exp(-(q/c)y + (A_l/c))$ then

$$g'(y) = -\frac{q}{c}\exp\left(-\frac{q}{c}y + \frac{A_l}{c}\right)\left[1 - \frac{q}{c}y\right]. \tag{116}$$

Using the properties of Lambert W function, we get

$$\begin{aligned}\left.\frac{dP(y_i^+)}{dy_i^+}\right|_{y_i^+=y^*} &= \left.\frac{d}{dy_i^+}\right|_{y_i^+=y^*}\left(-\frac{c}{q}W(g(y))\right)\\ &= -\frac{c}{q}\frac{W(g(y^*))}{1+W(g(y^*))}\left(\frac{1}{y^*} - \frac{q}{c}\right)\\ &= \frac{(y^*-\tau)(c-qy^*)}{y^*(c-q(y^*-\tau))}\\ &= h(y^*).\end{aligned} \tag{117}$$

It can be seen that if $y^* = (c/q) + \tau$ then $h(y^*) = -\infty$, and hence y^* is unstable. Thus, we will only consider the interval $[\tau, (c/q) + \tau)$. The fixed point is locally stable if $|h(y^*)| < 1$, which is equivalent to

$$-1 < \frac{(y^*-\tau)(c-qy^*)}{y^*(c-q(y^*-\tau))} < 1. \tag{118}$$

The right hand side inequality of (118) is obvious, so we only need to show the left hand side inequality, i.e.,

$$-1 < \frac{(y^*-\tau)(c-qy^*)}{y^*(c-q(y^*-\tau))}. \tag{119}$$

By simple calculations, we get

$$q(y^*)^2 - (c+q\tau)y^* + \frac{c\tau}{2} < 0, \tag{120}$$

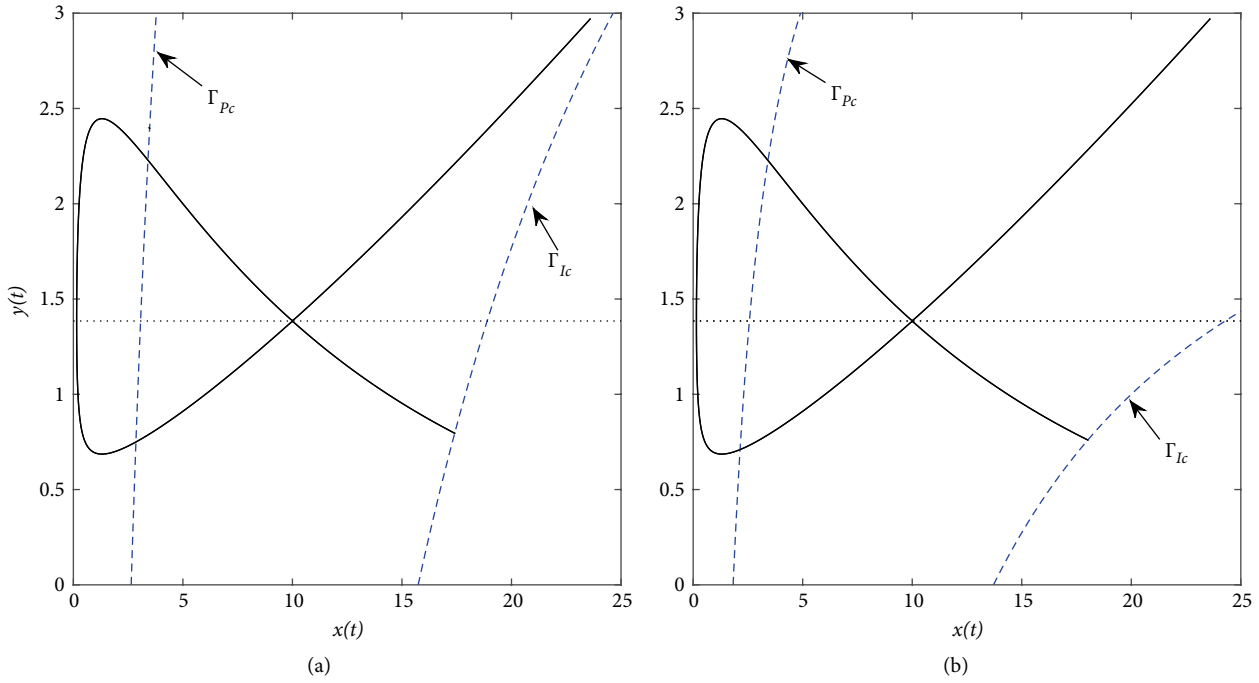

FIGURE 7: Effect of weighted parameters on Case (C_3). (a) $\beta = 0.1$, $A_l = 0.0088$, (b) $\beta = 0.3$, $A_l = -0.0279$. All other parametric values are fixed as: $c = 1.8, q = 1.3, \lambda = 0.52, \omega = 0.1, r = 0.23, \delta = 0.3, p = 0.8, \tau = 1.6, AT = 17$.

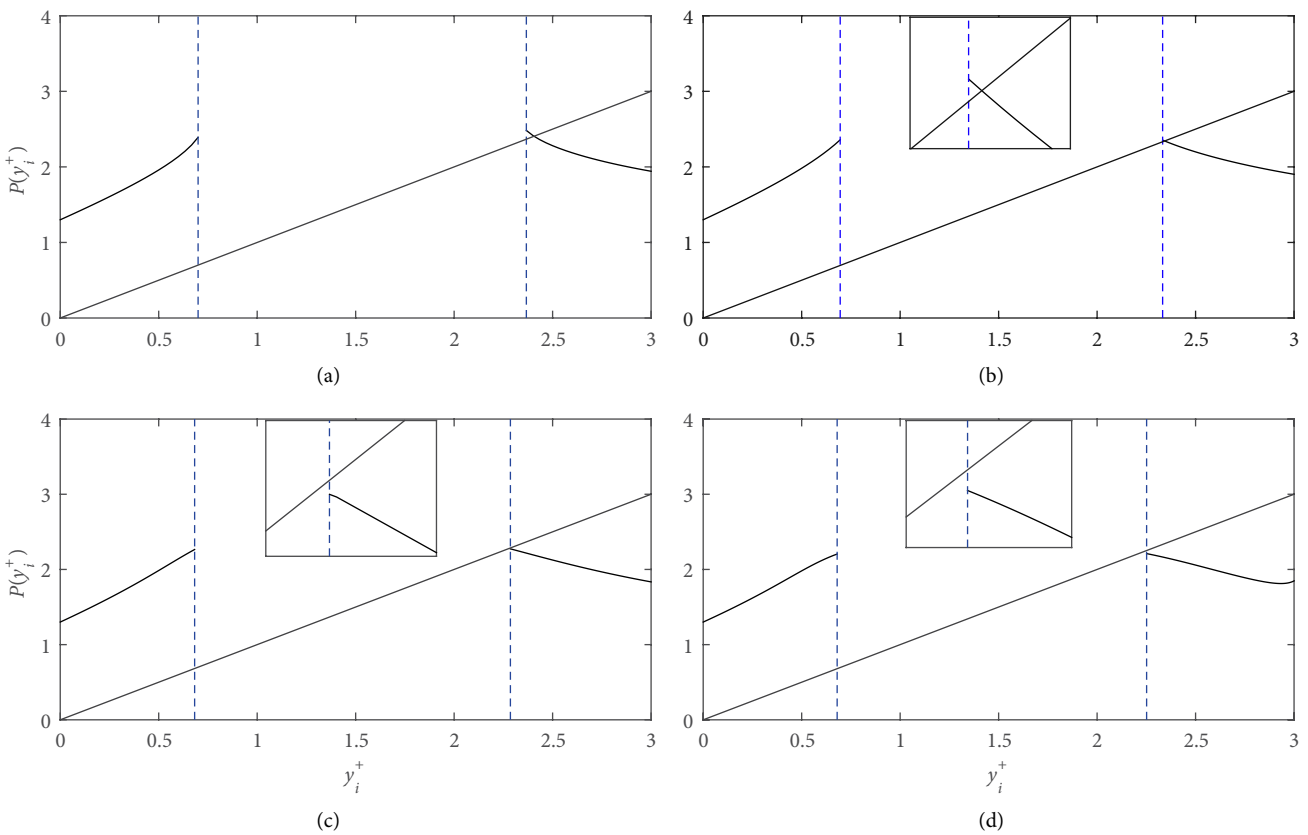

FIGURE 8: Effect of weighted parameters on the fixed point of Poincaré map for Case $(C_3)(i)$. (a) $\beta = 0$, (b) $\beta = 0.2$, (c) $\beta = 0.4$, (d) $\beta = 0.6$. All other parametric values are fixed as: $c = 1.8, q = 1.3, \lambda = 0.52, \omega = 0.1, r = 0.23, \delta = 0.3, p = 0.8, \tau = 1.3, AT = 12$.

and solving it with respect to y^*, we get

$$y_1^* = \frac{c + q\tau - \sqrt{c^2 + q^2\tau^2}}{2q} \quad \text{and} \quad y_2^* = \frac{c + q\tau + \sqrt{c^2 + q^2\tau^2}}{2q}. \tag{121}$$

It is obvious that $y_1^* < y^* < y_2^*$, and also we can easily show that $y_1^* < \tau < y_2^* < (c/q) + \tau$. This shows that if $\tau < y^* < y_2^*$, then for $A_l > 0$ the fixed point is locally stable. For case $A_l \le 0$, we already proved in Lemma 8 that $y^* < y_2^*$. This completes the proof. □

Corollary 4. *If $A_l > 0$ and $y^* > y_2^*$, then for model (2) the fixed point of Poincaré map is unstable.*

Corollary 5. *If $A_l^0 \le 0$, then for model (8) the fixed point of Poincaré map is locally stable. If $A_l^0 > 0$ and $y^* < y_2^*$, then the fixed point is locally stable, and it is unstable if $y^* > y_2^*$.*

For the global stability of the fixed point, based on the domains of the Poincaré map and Figure 5, we only focus on the Case (C_1) for $\tau > 0$ and have the following main result.

Theorem 7. *Suppose that for Case (C_1), the fixed point y^* of the Poincaré map $P(y_i^+)$ exists. Moreover, if*

(1) $P(y_S) < y_S$, then it is globally stable.

(2) $P(y_S) > y_S$, then it is globally stable given that $P^2(y^+) > y^+$ for $y^+ \in [y_S, y^*)$.

Proof. For Case (C_1), the existence of the fixed point is already discussed in Theorem 3. Here, we first prove that this fixed point is unique and later we check its global stability. From equation (56), we know that

$$y_{i+1}^+ = -\frac{c}{q} W\left[-\frac{q}{c} y_i^+ \left(\exp\left(-\frac{q}{c} y_i^+ + \frac{A_l}{c}\right)\right)\right] + \tau. \tag{122}$$

For the present case, we also know that $A_l \le 0$. If $y_S > y_0^+ > y_1^+ > \tau$ holds true, then from the monotonicity properties of Lambert W function and $g(y)$, the following relation must be fulfilled by the impulsive point sequence $\{y_k^+\}_{k=0}^{\infty}$:

$$y_S > y_0^+ > y_1^+ > \cdots > y_{k-1}^+ > y_k^+ > y_{k+1}^+ > \tau. \tag{123}$$

The domain of the Poincaré map justified that if $A_l \le 0$, then the above relation must be fulfilled by all the impulsive points. From which we can state that the impulsive point sequence is monotonically decreasing and it will converge to the unique constant $y^* \in [\tau, y_0^+)$, i.e., $\lim_{k\to\infty} y_k^+ = y^*$. The above discussion demonstrates that the fixed point is unique. The global stability of the fixed point can be presented as follows.

(1) If $P(y_S) < y_S$ and let $y_i^+ \in [0, y^*)$ then $y_i^+ < P(y_i^+) < y^*$. This shows that $P^k(y_i^+)$ for $k \ge 1$, is monotonically increasing and $\lim_{k\to\infty} P^k(y_i^+) = y^*$. Again let $y_i^+ \in (y^*, ((\alpha + c\beta)/q\beta) + \tau)$, then there are two possibilities: (i) for all k, we have $P^k(y_i^+) > y^*$. We know that in this interval $P(y_i^+) < y_i^+$, so $P^k(y_i^+)$ is monotonically decreasing and as a result, we can write $\lim_{k\to\infty} P^k(y_i^+) = y^*$; (ii) let $P^k(y_i^+) > y^*$ be not valid for all k, and let l_1 be the smallest positive integer such that $P^{l_1}(y_i^+) < y^*$. Then, by using the same method for $y_i^+ \in [0, y^*)$, if k is increasing then $P^{l_1+k}(y_i^+)$ is also monotonically increasing and $\lim_{k\to\infty} P^{l_1+k}(y_i^+) = y^*$. This shows that the result given in Case (1) is true.

(2) If $P(y_S) > y_S$, we take the following three intervals: $(a) y_i^+ \in [y_S, y^*), (b) y_i^+ \in [0, y_S), (c) y_i^+ \in (y^*, ((\alpha + c\beta)/q\beta) + \tau)$. For interval (a), the Poincaré map $P(y_i^+)$ is monotonically decreasing and hence for all $y_i^+ \in [y_S, y^*)$ we have $P(y_S) \ge P(y_i^+) > y^*$. Also applying the second condition $P^2(y_i^+) > y_i^+$, we get $y_i^+ < P^2(y_i^+) < y^*$ for all $y_i^+ \in [y_S, y^*)$. By induction, it is concluded that $P^{2(k-1)}(y_i^+) < P^{2k}(y_i^+) < y^*$ for all $k \ge 1$. This shows that $P^{2k}(y_i^+)$ is monotonically increasing with $\lim_{k\to\infty} P^{2k}(y_i^+) = y^*$.

For interval (b), the Poincaré map $P(y_i^+)$ is monotonically increasing, so there must exist $l_2 \ge 1$ such that either $P^{l_2}(y_i^+) > y^*$ or $P^{l_2}(y_i^+) \in [y_S, y^*)$. For the case, when $P^{l_2}(y_i^+) > y^*$ there must exist $\breve{y} \in [y_S, y^*)$ such that $P^{l_2}(y_i^+) = P(\breve{y})$, and hence $\lim_{k\to\infty} P^{l_2+2k}(y_i^+) = y^*$ monotonically. If $P^{l_2}(y_i^+) \in [y_S, y^*)$ then following the same way as in interval (a), we get $\lim_{k\to\infty} P^{l_2+2k}(y_i^+) = y^*$.

For interval (c), there exists a positive integer l_3 such that either $P^{l_3}(y_i^+) \in [0, y_S)$ or $[y_S, y^*)$. Hence, in the light of above intervals (a) and (b), it can be shown that the result given in Case (2) is true. This completes the proof of Theorem 7. □

Corollary 6. *For Case $(C_3)(ii)$, if $0 < \tau < \tau_4$, then there exists a unique fixed point for system (2) which is globally stable.*

7. Conclusion

Mathematical ecology is one of the basic elements of IPM process. It is the study of populations that interact, the way they affect the growth rates of each other. The Lotka–Volterra model is a very special case of such an interaction, in which there are two species, one of which is a prey and another one is a predator. Prey-predator models have received a high concentration of scholars due to their prosperous dynamic behavior. Prey and predator can impact each other's development, and such pairs exist throughout nature. It represents one of the primary models in mathematical ecology. Another fundamental concept of IPM process is that of using sound ET. It is the practical rule used to determine when to take management action.

In this paper, concerning IPM system, we have proposed and examined a commonly used prey-predator impulsive dynamical model with action threshold which depends on pest density and its change rate, which implies that the threshold is not only pest density dependent but also depends on the density of natural enemy. The threshold contains two weighted

quantities α and β. Once the weighted parameter β vanishes, i.e., $\beta = 0$ the action threshold just relies upon the density of pest population. Then the action threshold will be transformed into ET, which has been extensively demonstrated and explored in past writings [39–45].

The reason for choosing ratio-dependent AT is the presence of some practical issues in the previous used models during investigation on this topic. Firstly, for a comparatively large number of the pest population, its change rate is quite small. The second reason is that the number of population is small, but its change rate is significantly high which is more clear at the initial stage of the occurrence of the pest. Therefore, in order to overcome those shortcomings, we intended to take the model with action threshold depending on the pest density and its changing rate, which will result in complex curves for impulsive and phase sets.

Comparing with the main outcomes acquired for the prey-predator model in [46], we conclude that the ratio-dependent AT can altogether impact the dynamics of system proposed here including Poincaré map and fixed point, which is very useful for structuring proper pest control measures. The complex and rich dynamics occur when model (2) does not exist the fixed point of Poincaré map. Moreover, the increasing and extensive uses of systems with ratio-dependent AT as control measures in a wide variety of fields require much more advanced and new qualitative techniques to explore their whole dynamics and reveal the important biological implications. This is an enormous task for analyzing the system with ratio-dependent AT, and new methodologies need to be established.

Applying the Lambert W function function and its properties, the exact impulsive and phase sets were found. Based on these, the Poincaré map is shaped for the exact phase set. The conditions for the existence and stability of the boundary order-1 periodic solution are provided. From Figure 4, it can be seen that the numerical simulation also agrees with the theoretical outcomes. Sufficient conditions that confirm the order-1 periodic solution and its stability were studied. It is also studied in detail how and under what conditions the fixed point of Poincaré map and its stability are affected by the weighted parameters α and β.

Figures 5, 6, and 8 demonstrate that the definition domain of the Poincaré map is indeed very complex for system (2). Numerical simulation shows how the shapes of Poincaré map vary with the small changes in the weighted parameters α and β. The fixed point of the Poincaré map, i.e., periodic solution of order-1 is affected by the weighted parameters. If the weighted parameter β increases, for some cases it decreases monotonically and for some cases it increases monotonically. For those cases where the fixed point is increasing, we get its minimum value whenever $\beta = 0$, i.e., the threshold relies upon the pest density, as shown in Figure 5. For those cases where the fixed point is decreasing, we get its maximum value whenever $\beta = 0$, as shown in Figure 8.

The new investigative procedures built up in this paper could not easily be applied to other generalized models with state-dependent feedback control [50–53], yet also can assist us in comprehending further the qualitative behavior of the planar impulsive semidynamical system and encourage us to address more extensive issues. Compared with the previous work, we provided the exact domains for impulsive and phase sets. We believe that the idea of action threshold is more general and practical as it depends on pest density and its change rate. It also can generate new significant directions as compared with those introduced in previous studies.

We considered the more general pest and natural enemy systems with ratio-dependent AT, and no doubt it is crucial to determine the Poincaré map and analyze the global dynamics. The impulsive and phase sets are complex curves rather than straight lines. The main results of this paper exhibit that the pests can be entirely controlled by applying control action for a predetermined number of times such that the ratio-dependent AT is not exceeded. Numerical simulation additionally illustrates another essential reality that the impulsive and phase sets not just change with the change of the weight parameters α and β, yet also rely upon the interaction between the pest and its natural enemy.

Data Availability

No data were used to supposed this study.

Conflicts of Interest

The authors declare that they have no conflicts of interest.

Acknowledgments

This work was supported by the National Natural Science Foundation of China (61772017, 11631012), and by the Fundamental Research Funds for the Central Universities (GK201901008).

References

[1] D. Mahr, P. Whitaker, and N. Ridgway, *Biological Control of Insects and Mites: An Introduction to Beneficial Natural Enemies and Their Use in Pest Management*, National Agricultural Library Information Systems Division, 1993.

[2] D. Hueth and U. Regev, "Optimal agricultural pest management with increasing pest resistance," *American Journal of Agricultural Economics*, vol. 56, no. 3, pp. 543–552, 1974.

[3] M. E. Whalon, D. M. Sanchez, and R. M. Hollingworth, *Global Pesticide Resistance in Arthropods*, Commonwealth Agricultural Bureaux International, Cambridge, 2008.

[4] L. E. Ehler, "Integrated pest management (IPM): definition, historical development and implementation, and the other IPM," *Pest Management Science*, vol. 62, no. 9, pp. 787–789, 2006.

[5] M. R. Hardin, B. Benrey, M. Coll, W. O. Lamp, G. K. Roderick, and P. Barbosa, "Arthropod pest resurgence: an overview of potential mechanisms," *Crop Protection*, vol. 14, no. 1, pp. 3–18, 1995.

[6] R. F. Smith and H. T. Reynolds, "Principles, definitions and scope of integrated pest control, Food and Agriculture Organization of the United Nations," 1966.

[7] "United states department of agriculture," 2015, http://www.ars.usda.gov.

[8] J. C. Van Lenteren, "Integrated pest management in protected crops," *D. Dent Integrated Pest Management*, pp. 311–343, Chapman Hall, London, 1995.

[9] J. C. Van Lenteren, "Environmental manipulation advantageous to natural enemies of pests," in *Integrated Pest Management Parasitis*, V. Delucchi, Ed., pp. 123–166, Geneva, 1987.

[10] S. Y. Tang, Y. N. Xiao, L. S. Chen, and R. A. Cheke, "Integrated pest management models and their dynamical behaviour," *Bulletin of Mathematical Biology*, vol. 67, no. 1, pp. 115–135, 2005.

[11] Y. N. Xiao and F. Van Den Bosch, "The dynamics of an eco-epidemic model with biological control," *Ecological Modelling*, vol. 168, no. 1-2, pp. 203–214, 2003.

[12] H. J. Barclay, "Models for pest control using predator release, habitat management and pesticide release in combination," *Journal of Applied Ecology*, vol. 19, no. 2, pp. 337–348, 1982.

[13] S. Y. Tang and L. Chen, "Modelling and analysis of integrated pest management strategy," *Discrete and Continuous Dynamical Systems - Series B*, vol. 4, no. 3, pp. 759–768, 2004.

[14] B. Liu, L. S. Chen, and Y. J. Zhang, "The dynamics of a prey-dependent consumption model concerning impulsive control strategy," *Applied Mathematics and Computation*, vol. 169, no. 1, pp. 305–320, 2005.

[15] S. Y. Tang, G. Y. Tang, and R. A. Cheke, "Optimum timing for integrated pest management: modelling rates of pesticide application and natural enemy releases," *Journal of Theoretical Biology*, vol. 264, no. 2, pp. 623–638, 2010.

[16] S. Y. Tang, J. Liang, Y. Tan, and R. A. Cheke, "Threshold conditions for integrated pest management models with pesticides that have residual effects," *Journal of Mathematical Biology*, vol. 66, no. 1-2, pp. 1–35, 2013.

[17] V. Lakshmikantham, D. D. Bainov, and P. S. Simeonov, *Theory of Impulsive Diferential Equations*, World Scientific, Singapore, 1989.

[18] P. Wang, W. Qin, and G. Tang, "Modelling and analysis of a host-parasitoid impulsive ecosystem under resource limitation," *Complexity*, vol. 2019, Article ID 9365293, 12 pages, 2019.

[19] X. Song and Z. Xiang, "The prey-dependent consumption two-prey one-predator models with stage structure for the predator and impulsive effects," *Journal of Theoretical Biology*, vol. 242, no. 3, pp. 683–698, 2006.

[20] H. Zhang, P. Georgescu, and L. Chen, *An Impulsive Predator–Prey Model of Integrated Pest Management*, CEU, Department of Mathematics, 2007.

[21] P. Georgescu, H. Zhang, and L. Chen, "Bifurcation of nontrivial periodic solutions for an impulsively controlled pest management model," *Applied Mathematics and Computation*, vol. 202, no. 2, pp. 675–687, 2008.

[22] J. Jiao and L. Chen, "Global attractivity of a stage-structure variable coefficients predator-prey system with time delay and impulsive perturbations on predators," *International Journal of Biomathematics*, vol. 1, no. 2, pp. 197–208, 2008.

[23] B. Liu, Y. Zhang, and L. Chen, "Dynamic complexity in Lotka–Volterra predator-prey system concerning impulsive control strategy," *International Journal of Bifurcation and Chaos*, vol. 15, no. 2, pp. 517–531, 2005.

[24] B. Liu, Y. Zhang, L. Chen, and L. Sun, "The dynamics of a prey-dependent consumption model concerning integrated pest management," *Acta Mathematica Sinica*, vol. 21, no. 3, pp. 541–554, 2005.

[25] Y. Pei, X. Ji, and C. Li, "Pest regulation by means of continuous and impulsive nonlinear controls," *Mathematical and Computer Modelling*, vol. 51, no. 5-6, pp. 810–822, 2010.

[26] S. Y. Tang, R. A. Cheke, and Y. N. Xiao, "Effects of predator and prey dispersal on success or failure of biological control," *Bulletin of Mathematical Biology*, vol. 71, no. 8, pp. 2025–2047, 2009.

[27] J. Yang and S. Y. Tang, "Effects of population dispersal and impulsive control tactics on pest management," *Nonlinear Analysis: Hybrid Systems*, vol. 3, no. 4, pp. 487–500, 2009.

[28] H. Zhang, J. Jiao, and L. Chen, "Pest management through continuous and impulsive control strategies," *Biosystems*, vol. 90, no. 2, pp. 350–361, 2007.

[29] Z. Xiang, S. Tang, C. Xiang, and H. Wu, "On impulsive pest control using integrated intervention strategies," *Applied Mathematics and Computation*, vol. 269, pp. 930–946, 2015.

[30] Y. Tian, S. Y. Tang, and R. A. Cheke, "Dynamic complexity of a predator-prey model for IPM with nonlinear impulsive control incorporating a regulatory factor for predator releases," *Mathematical Modelling and Analysis*, vol. 24, no. 1, pp. 134–154, 2019.

[31] X. Wang, Y. Tian, and S. Y. Tang, "A holling type II pest and natural enemy model with density dependent IPM strategy," *Mathematical Problems in Engineering*, vol. 2017, Article ID 8683207, 12 pages, 2017.

[32] S. Y. Tang and R. A. Cheke, "Models for integrated pest control and their biological implications," *Mathematical Biosciences*, vol. 215, no. 1, pp. 115–125, 2008.

[33] S. Y. Tang, Y. N. Xiao, and R. A. Cheke, "Multiple attractors of host–parasitoid models with integrated pest management strategies: eradication, persistence and outbreak," *Theoretical Population Biology*, vol. 73, no. 2, pp. 181–197, 2008.

[34] J. Yang and S. Y. Tang, "Holling type II predator-prey model with nonlinear pulse as state-dependent feedback control," *Journal of Computational and Applied Mathematics*, vol. 291, pp. 225–241, 2016.

[35] S. Tang, X. Tan, J. Yang, and J. Liang, "Periodic solution bifurcation and spiking dynamics of impacting predator–prey dynamical model," *International Journal of Bifurcation and Chaos*, vol. 28, no. 12, Article ID 1850147, 2018.

[36] J. C. V. Lenteren, "Success in biological control of arthropods by augmentation of natural enemies," *Biological Control: Measures of Success*, pp. 77–103, Springer, Netherlands, 2000.

[37] M. L. Flint, *Integrated Pest Management for Walnuts, Division of Agricultural sciences, Agriculture and Natural Resources*, pp. 36–41, University of California Statewide Integrated Pest Management Project, 2nd edition, 1987.

[38] L. P. Pedigo, *Entomology and Pest Management*, 679 pages, Prentice Hall, Upper Saddle River, NJ, 2nd edition, 1996.

[39] J. Wang, H. Cheng, X. Meng, and B. G. S. A. Pradeep, "Geometrical analysis and control optimization of a predator–prey model with multi state-dependent impulse," *Advances in Difference Equations*, vol. 2017, no. 1, Article ID 252, 2017.

[40] Q. Xiao and B. Dai, "Periodic solutions generated by impulses for state-dependent impulsive differential equation," *Discrete Dynamics in Nature and Society*, vol. 2015, Article ID 816325, 7 pages, 2015.

[41] S. Y. Tang and R. A. Cheke, "State-dependent impulsive models of integrated pest management (IPM) strategies and their dynamic consequences," *Journal of Mathematical Biology*, vol. 50, no. 3, pp. 257–292, 2005.

[42] L. Feng and Z. Liu, "An impulsive periodic predator-prey Lotka–Volterra type dispersal system with mixed functional responses," *Journal of Applied Mathematics and Computing*, vol. 45, no. 1-2, pp. 235–257, 2014.

[43] T. Zhang, W. Ma, X. Meng, and T. Zhang, "Periodic solution of a prey-predator model with nonlinear state feedback control," *Applied Mathematics and Computation*, vol. 266, pp. 95–107, 2015.

[44] Y. F. Li, D. L. Xie, and J. A. Cui, "Complex dynamics of a predator–prey model with impulsive state feedback control," *Applied Mathematics and Computation*, vol. 230, pp. 395–405, 2014.

[45] T. Zhang, J. Zhang, X. Meng, and T. Zhang, "Geometric analysis of a pest management model with Holling's type III functional response and nonlinear state feedback control," *Nonlinear Dynamics*, vol. 84, no. 3, pp. 1529–1539, 2016.

[46] S. Y. Tang, W. H. Pang, R. A. Cheke, and J. H. Wu, "Global dynamics of a state-dependent feedback control system," *Advances in Difference Equations*, vol. 2015, no. 1, Article ID 322, 2015.

[47] I. U. Khan, S. Y. Tang, and B. Tang, "The state-dependent impulsive model with action threshold depending on the pest density and its changing rate," *Complexity*, vol. 2019, Article ID 6509867, 15 pages, 2019.

[48] P. Simeonov and D. Bainov, "Orbital stability of periodic solutions of autonomous systems with impulse effect," *International Journal of Systems Science*, vol. 19, no. 12, pp. 2561–2585, 1988.

[49] D. Bainov and P. Simeonov, *Impulsive Differential Equations, Periodic Solutions and Applications, Monographs and Surveys in Pure and Applied Mathematics*, Longman Scientific and Technical, New York, 1993.

[50] B. Liu, Y. Tian, and B. L. Kang, "Dynamics on a Holling II predator-prey model with state-dependent impulsive control," *International Journal of Biomathematics*, vol. 5, no. 3, pp. 1–18, 2012.

[51] S. Y. Tang, B. Tang, A. L. Wang, and Y. N. Xiao, "Holling II predator-prey impulsive semi-dynamic model with complex Poincare map," *Nonlinear Dynamics*, vol. 81, no. 3, pp. 1575–1596, 2015.

[52] Y. Tian, K. B. Sun, A. Kasperski, and L. S. Chen, "Nonlinear modelling and qualitative analysis of a real chemostat with pulse feeding," *Discrete Dynamics in Nature and Society*, vol. 2010, Article ID 640594, 18 pages, 2010.

[53] Y. Tian, S. Y. Tang, and R. A. Cheke, "Nonlinear state-dependent feedback control of a pest-natural enemy system," *Nonlinear Dynamics*, vol. 94, no. 3, pp. 2243–2263, 2018.